Clim. Past Discuss., 8, 4817–4883, 2012
www.clim-past-discuss.net/8/4817/2012/
doi:10.5194/cpd-8-4817-2012


Climate of the Past Discussions



# Causes of Greenland temperature variability over the past 4000 yr: implications for northern hemispheric temperature change

**T. Kobashi[1,2], K. Kawamura[1], K. Goto-Azuma[1], J. E. Box[3], C.-C. Gao[4], and T. Nakaegawa[5]**

[1]National Institute of Polar Research, 10-3 Midoricho, Tachikawa, Tokyo 190-8518, Japan
[2]Scripps Institution of Oceanography, University of California, San Diego, La Jolla, CA, USA
[3]Byrd Polar Research Center, Ohio State University, Columbus, Ohio, USA
[4]Zhejiang University, Hangzhou, Zhejiang, China
[5]Meteorological Research Institute, Tsukuba, Ibaraki 305-0052 Japan

Received: 10 September 2012 – Accepted: 22 September 2012 – Published: 28 September 2012

Correspondence to: T. Kobashi (kobashi.takuro@nipr.ac.jp)

Published by Copernicus Publications on behalf of the European Geosciences Union.

## Abstract

A new Greenland temperature record reconstructed from argon and nitrogen isotopes from trapped air in a GISP2 ice core, provides high-resolution (< 20 yr) and precise annual average temperature estimates for the past 4000 yr. Due to tight age-controls and abundant paleoclimatic information from the ice core, the temperature record provides an exceptional opportunity to investigate the late Holocene climate in a multi-decadal to millennial time scale. To investigate causes of Greenland temperature variability over the past 4000 yr, we calculated high latitude (70–80° N) temperature change using a one-dimensional energy balance model with reconstructed climate forcings including orbital, solar, volcanic, and greenhouse gas forcings. Greenland temperature was calculated from the high latitude temperature, considering Greenland's negative temperature responses to solar variability due to associated changes in atmospheric and oceanic circulations. The calculated Greenland temperature was significantly correlated with the ice-core-derived Greenland temperatures with the 97 % confidence level. Therefore, the past variability of climate forcings can explain at least 10 % of the multi-decadal to millennial variability in Greenland temperature over the past 4000 yr. An average temperature trend for the Northern Hemisphere (NH) over the past 4000 yr was also inferred from the ice-core derived Greenland temperatures. Lines of evidence indicate that the current decadal average temperature of NH is likely warmer than at any time over the past 4000 yr. Sequential cooling events starting around 800 B.C.E. (the 2.8 ka event), which were induced by several large volcanic eruptions as well as low solar activity, had similar magnitude with the Little Ice Age cooling.

## 1 Introduction

Human society has experienced remarkable development over the past 4000 yr under a changing climate. Understanding climate variability over this period is therefore critical to the investigation of the relationship between climate change and human society.

As climate boundary conditions (e.g. areas covered by ice sheets and global sea-level) over the past 4000 yr were largely similar to those of the present, this period provides a baseline on which future human-induced climate change is expected to occur (Crowley and North, 1996). However, studies have indicated that global to hemispheric average temperatures on multi-decadal to centennial time scales can only be reasonably estimated from temperature proxies over the past 1000–2000 yr, due to uncertainties in calibrations and chronologies (North et al., 2006; Mann et al., 2008; Moberg et al., 2005). These studies have shown that the current hemispheric average temperature is likely warmer than at any time over the past 2000 yr, but it is still unknown whether the present temperature level has ever been reached over the past 4000 yr and how it varied regionally. High latitude regions, including Greenland, are some of the most important areas for determining the impacts of future climate change, as these regions are expected to experience large changes owing to polar amplification and the substantial influence that the melting of the Greenland ice sheet has on global coastal areas due to sea level rise (Jacob et al., 2012).

Many paleo-temperature proxies are biologically mediated, generally recording summer to spring temperatures (Kaufman et al., 2004, 2009), and often the relationships between climatic and biological parameters are not stationary (Huntley, 2011). To derive hemispheric to global average temperatures on a multi-decadal to centennial time scale, temperature proxies with large uncertainties in temperature and chronology are compiled such that the multi-decadal to centennial trends are frequently smoothed out, with the trends increasing as they go further back in time (Wanner et al., 2008). Therefore, we explored a new way to infer a hemispheric temperature trend from a Greenland temperature record (Kobashi et al., 2011) that possesses high accuracy and tight age controls. This possible only after the regional climatic anomaly from the global trend was understood (Kobashi et al., 2012). We note that Greenland temperatures have three advantages in this regard: first, annually layered ice cores are available; second, it is located near the center of the Northern Hemisphere (NH); and finally, hemispheric temperature signals are intensified by polar amplification.

Greenland temperature over the past 4000 yr was estimated using argon and nitrogen isotopes from trapped air in the GISP2 ice core (Kobashi et al., 2008b, 2010, 2011). The multi-millennial trend was constrained using the borehole temperature profile (Kobashi et al., 2011). The temperature estimates are decadal averages of mean "annual" temperatures (10–20 yr in Central Greenland, Spahni et al., 2003) as heat and gas diffusion in the firn layer (unconsolidated permeable snow layer) smoothes large seasonal and inter-annual temperature variations (Severinghaus et al., 1998). As it is constrained by a physical process, the record's accuracy for multi-decadal to centennial temperature changes over the past 4000 yr is arguably among the highest of all of the paleo-temperature proxies, which are generally affected by large seasonal temperature changes and associated climate variables.

In this study, we investigated the causes of Greenland temperature changes over the past 4000 yr using a new Greenland temperature record (Kobashi et al., 2011) by employing a climate model with reconstructed climate forcings; and we explored the corresponding implications for temperature changes in the NH. In Sect. 2, we describe the chronology of the temperature record and the methods of analysis. In Sect. 3, we present our investigation of how Greenland Summit temperatures relate to other parts of Greenland and the world. Additionally, we compared the Greenland temperature record with oxygen isotope records ($\delta^{18}O_{ice}$) from six Greenland ice cores. In Sect. 4, we discuss the solar influence on the Greenland temperatures and $\delta^{18}O_{ice}$ over the past 4000 yr, based on the theory we developed for the Greenland temperatures over the past 800 yr (Kobashi et al., 2012). In Sect. 5, we present the climate forcings that were developed and applied to a one-dimensional energy balance model. Finally, we investigated the causes of the variation of Greenland temperature and implications for the NH temperature trend over the past 4000 yr.





CPD
8, 4817–4883, 2012

## 2 Methods

### 2.1 Ice core chronology

The "visual stratigraphy" chronology (Alley et al., 1997) was used for the various data from the GISP2 ice core, which allowed us to compare temperature changes to other climatic information in the ice core with minimum age uncertainties (e.g. GISP2 $\delta^{18}O_{ice}$ and sulfate for volcanic signals). The uncertainty of the chronology has been estimated to be 1 % (Alley et al., 1997). The ages of gas and ice differ in ice cores because the age of the gas is determined at the time of bubble closure at the bottom of the snow layer. Differences between gas age and ice age were estimated using a firn-densification/heat diffusion model (Goujon et al., 2003). Uncertainty in the differences is approximately 10 %, or approximately 20 yr, as the gas age to ice age differences are approximately 200 yr in Central Greenland during the Holocene (Goujon et al., 2003). The uncertainty estimate is likely conservative as timings of the changes in $\delta^{18}O_{ice}$ and temperature agree well (Kobashi et al., 2010). Therefore, absolute age uncertainties are less than 45 yr at approximately 2000 B.C.E. (= $\sqrt{40^2+20^2}$; from the theory of error propagation) and less than 20 yr at approximately 1950 C.E. Comparison with the GICO05 chronology (Vinther and Rasmussen, personal communication, 2012) indicates that these are appropriate estimates. The use of the GICO05 chronology had little effect on the following analyses, as the differences between GICO05 and visual stratigraphy are relatively small over the past 4000 yr. The data produced in this paper, including a depth scale of the temperature record, will be deposited at the NOAA paleoclimate web site (http://www.ncdc.noaa.gov/paleo/data.html) after publication.

### 2.2 Correlation coefficients and significance

The Pearson product-moment correlation coefficient was calculated to evaluate the strength of the correlations. Because of the autocorrelations of the time series, it is important to consider the reduced degree of freedom for the calculation of significance.



CPD
8, 4817–4883, 2012

The number of effective degrees of freedom ($df_e$) for $p$ statistics was estimated from the effective sample size ($N_e$), which depends on the effective decorrelation time ($T_e$) (Ito and Minobe, 2010). The two relevant time series are represented by $X$ and $Y$, and the sample size is $N$. Here, the time interval ($\Delta t$) is 1 yr. Therefore, $N_e = N\Delta t/T_e$ and $df_e = N_e - 2$. For the correlation coefficients, $T_e$ is estimated as $T_e = \Delta t \sum_{\tau=-N}^{N} (\rho_{XX}(\tau)\rho_{YY}(\tau) + \rho_{XY}(\tau)\rho_{YX}(\tau))$, where $\tau$ is a lag or lead in years, and $\rho$ is the correlation coefficient of the 2 time series indicted by the subscripts ($XX$ and $YY$ are autocorrelations) (Ito and Minobe, 2010). The range of $\Sigma(-N, N)$ was defined as $\rho$ becomes zero, with $\tau$ starting from zero and moving to an increased lag or lead with a 1 yr time step. Then, $p$-values of the correlation coefficients were calculated from a two-sided Student's t-distribution with the effective samples size ($N_e$) described above. We considered a 90 % confidence level ($p = 0.1$) as a significant correlation but reported all $p$-values where $p$ is less than 0.1.

## 3 Greenland temperature

### 3.1 Greenland temperatures over the past 4000 yr

There have been several attempts to reconstruct the variability of Greenland temperature, which have included the use of classic methods of application of oxygen isotopes of ice ($\delta^{18}O_{ice}$) (Dansgaard, 1964; Vinther et al., 2010; Johnsen et al., 2001; White et al., 1997; Jouzel et al., 1997), borehole thermometry (Alley and Koci, 1990; Dahl-Jensen et al., 1998), and combinations of the two techniques (Cuffey and Clow, 1997; Cuffey et al., 1995). However, $\delta^{18}O_{ice}$ is known to be affected by factors other than local temperature change, such as changes in storm tracks, seasonal accumulation, vapor-source temperature, and the location of evaporative origins (LeGrande and Schmidt, 2009; Masson-Delmotte et al., 2005; Steen-Larsen et al., 2011; Charles et al., 1994). Physically constrained borehole thermometry is more accurate but it loses information on shorter-term temperature variation rather quickly (Dahl-Jensen et al., 1998).

Recently, Vinther et al. (2009) reconstructed Greenland temperature variations from $\delta^{18}O_{ice}$ and borehole temperature profiles, while considering changes in ice-sheet elevation.

Greenland temperature record for the past 4000 yr has been developed (Kobashi et al., 2010, 2011) using nitrogen and argon isotopes from trapped air in ice cores (Kobashi et al., 2008b). Gasses in the firn layer (unconsolidated permeable snow layer) fractionate according to the depth of the layer (gravitational fraction) and the temperature gradient ($\Delta T$; thermal fractionation) in the layer (Severinghaus et al., 1998). Therefore, previous information on firn depths and temperature gradients can be obtained by measuring two isotope ratios from trapped air in ice cores (e.g. nitrogen and argon) as deviations from present values in the atmosphere (Severinghaus et al., 1998; Kobashi et al., 2008b). This method has been applied to quantify the magnitudes of abrupt climate changes by calibrating $\delta^{18}O_{ice}$ to match measured nitrogen and argon isotopes (Kobashi et al., 2007; Severinghaus and Brook, 1999; Severinghaus et al., 1998; Landais et al., 2004; Lang et al., 1999; Huber et al., 2006).

As $\delta^{18}O_{ice}$ may not reflect local temperature changes, especially for periods such as the relatively stable Holocene, it was necessary to develop a new method to calculate surface temperatures directly from nitrogen and argon isotopes without relying on $\delta^{18}O_{ice}$. For this purpose, we developed a method (Kobashi et al., 2008a, 2010, 2011) to calculate surface temperature change directly by integrating $\Delta T$ (derived from nitrogen and argon isotopic data) with a firn densification/heat diffusion model (Goujon et al., 2003). We note that the reconstructed temperature records for the past 1000 yr reported in Kobashi et al. (2010) and in Kobashi et al. (2011) are nearly identical, but are slightly different owing to differences in temperature histories prior to 1000 C.E. in the models (Fig. 1). Greenland temperature record for the past 4000 yr (Kobashi et al., 2011) was reconstructed for a longer temperature history with better agreement with borehole temperature profiles than in Kobashi et al. (2010); therefore, it should be more consistent with actual temperature changes. The reconstructed Summit temperatures over the past 160 yr (Kobashi et al., 2011) closely match independently reconstructed

Summit temperatures from observation and climate model (Box et al., 2009) within uncertainties (Kobashi et al., 2011).

### 3.2 Spatial correlation between Summit temperatures and other areas of Greenland and the world

The Greenland temperature record (Kobashi et al., 2011) was derived from the GISP2 ice core from the Summit region of Central Greenland. To make inferences about the past, it is critical to understand how the Summit temperature is connected with other parts of Greenland and the world. The relationship with the NH temperature trend was investigated thoroughly in Kobashi et al. (2012). Box et al. (2009) produced Greenland grid temperatures from 1840 to 2007 (now updated to 2011). Using the grid temperatures, two correlation maps were created for the period of 1852–2010 (a period for which continuous data are available) for the two reconstructed Summit temperatures. One Summit record is derived from the ice core by Kobashi et al. (2011), and the other is from a fusion of observations and a climate model by Box et al. (2009). The Summit temperature by Box et al. (2009) is the same as that used by Kobashi et al. (2011). The correlation map with the observation-based data by Box et al. (2009) shows a higher correlation with the grids in general than the record from Kobashi et al. (2011) likely because the observation-based Summit temperature is more precise. Therefore, we used the correlation map with the Box et al. Summit temperatures for further discussion. However, we note that both maps share similar characteristics (Fig. 2).

East Greenland exhibits higher correlations, and the northern coastal areas also exhibit relatively high correlations. However, Northwest and South Greenland exhibit lower correlations with the Summit temperature, reflecting regional climatic patterns. The grid temperatures in most of Greenland are highly correlated with the Summit temperatures, as the 5th percentile of all the grid correlation coefficients is $r = 0.73$ (Fig. 2, top), indicating that 95 % of the grid correlation coefficients are higher than $r = 0.73$. This is in line with the fact that the observation-based Summit temperature is highly correlated ($r = 0.92$; $p < 0.01$) with the average Greenland ice-sheet surface





CPD
8, 4817–4883, 2012

air temperature calculated by Box et al. (2009) (Kobashi et al., 2012). Therefore, the Summit temperature record should be a useful indicator of the melting of the ice sheet in coastal regions in the past, and consequently changes in the Greenland ice sheet.

To further extend our inferences of the Summit temperature, we examined correlation maps between the Greenland Summit temperatures (Box et al., 2009; Kobashi et al., 2011) and global grid surface air temperatures (GISS) (Hansen et al., 2010) for the period from 1880–2010 (Fig. 3). As with the Greenland correlation maps, two Summit temperature estimates from Box et al. (2009) and Kobashi et al. (2011) were used (Fig. 4). Both maps generally exhibit similar teleconnection patterns, but the map with the Box et al. Summit temperature shows higher correlations with the grid temperatures (Fig. 3), as was observed with the Greenland maps. Therefore, we further examined the correlation map with the Box et al. Summit temperatures, as it contains inter-annual temperature variability. The correlation map indicates a significantly high positive correlation with the Northern North Atlantic, Western Mediterranean, Middle East, and Northern Africa, resembling one of the two regimes of the NAO/AO (North Atlantic Oscillation/Arctic Oscillation) dipole pattern (Marshall et al., 2001; Hurrell, 1995). Some tropical regions of the Atlantic, Indian, and Pacific Ocean, where the NAO has been linked with tropical dynamics (Hurrell et al., 2003), also exhibit high correlation.

Interestingly, very high correlations ($r = 0.7$ to 0.80) are found in geographically distant regions such as the tropical Atlantic, Eastern Mediterranean, and Middle East (Red Sea and Persian Gulf), with correlations as high as near Iceland, indicating strong teleconnective patterns for these regions with Greenland over the past 130 yr (Fig. 3). The link between the Greenland temperature and Mediterranean temperature (including the Middle East) may provide a clue for early cultural changes in the Middle East (Kobashi, 2007; Kobashi et al., 2011). One exception from the NAO pattern is located in the mid latitudes of North America, which is usually identified as part of the other side of the NAO dipole. This may be explained by the fact that the climate of the region is also affected by the Atlantic Multi-decadal Oscillation (AMO) (Enfield et al., 2001; McCabe et al., 2004). The general spatial patterns of the correlation over the past





CPD
8, 4817–4883, 2012

130 yr were also indentified in a correlation map between the grid proxy temperatures (Mann et al., 2009) and Greenland temperatures (Kobashi et al., 2011) over the past 800 yr (Fig. 3), indicating that the general atmospheric and oceanic circulation pattern connecting Greenland and other parts of the world for the past 130 yr has been active for the past 800 yr (Fig. 3).

The temperature trend in West Iceland (Reykjavik) exhibits a similar pattern to East Greenland (Tasiilaq) over the past 130 yr, with both showing a negative correlation with the NAO index (Hanna et al., 2004). The strong association of the temperature trends between East Greenland and West Iceland can be inferred from the Greenland and global correlation maps (Figs. 2 and 3). As large areas of the North Atlantic and the Summit temperatures exhibit high correlations except around the storm track region (Fig. 3), the North Atlantic average temperatures (Enfield et al., 2001) and the Summit temperatures (Box et al., 2009) are highly correlated ($r = 0.58$, $p = 0.03$ as in Fig. 4). Multi-decadal variation (21-yr running means; RMs) of the Summit temperature (Box et al., 2009) can explain 70 % of the variance in the North Atlantic average temperatures (Enfield et al., 2001). Thus, the Summit temperature is highly influenced by the Atlantic Multi-decadal Oscillation (AMO) (Enfield et al., 2001), which is a climate mode of variability with an approximate periodicity of 70 yr and that has global impacts (Dima and Lohmann, 2007). The causes of the oscillation have been associated with the internal oscillation of the Atlantic Meridional Overturning Circulation (AMOC) possibly influenced by solar variation and volcanic eruptions (Knudsen et al., 2011; Otterå et al., 2010). Greenland temperature variability over the past 4000 yr (Kobashi et al., 2011) contains a fairly persistent periodicity of approximately 70 yr (Fig. 5), indicating the consistent nature of the AMO over the past 4000 yr (Chylek et al., 2012; Knudsen et al., 2011). Notably, in the following sections, we identified parts of the causes of Greenland temperature over the past 4000 yr, which must be linked with the causes of variability in the AMO.





CPD
8, 4817–4883, 2012

### 3.3 Greenland temperatures and oxygen isotopes over the past 4000 yr

Oxygen isotopes of ice ($\delta^{18}O_{ice}$) have been widely used as temperature proxies in Greenland. However, it is known that $\delta^{18}O_{ice}$ is affected by many other climatic processes (LeGrande and Schmidt, 2009; Johnsen et al., 2001; Vinther et al., 2010; Steen-Larsen et al., 2011). With the independent temperature record on hand, we can evaluate $\delta^{18}O_{ice}$ records as a temperature proxy over the past 4000 yr. Based on the high correlations between the Summit temperatures and most of the Greenland grid temperatures over the past 159 yr (Fig. 2), we expect that actual temperature trends at each core site were strongly correlated over the past 4000 yr. In addition, elevational changes of the Greenland ice sheet were likely at a minimum over the past 4000 yr (e.g. < 100 m) and therefore should be a limited source of the different temperature trends observed in different parts of the Greenland ice sheet (Vinther et al., 2009).

$\delta^{18}O_{ice}$ records of six ice cores from the Greenland region (GISP2, GRIP, Agassiz, NGRIP, Renland, and Dye-3; Fig. 6 and Table 1) were compared with the temperature record (Kobashi et al., 2011). The observation that $\delta^{18}O_{ice}$ of the GISP2 ice core has a lower correlation with Greenland temperatures than that of other cores, although the temperature was derived from the same GISP2 ice core (Kobashi et al., 2011), is evidence of the influence of nonlocal temperature factors on $\delta^{18}O_{ice}$. The correlation coefficients between temperature and $\delta^{18}O_{ice}$ are ranked in the following order: NGRIP ($r = 0.39$, $p = 0.01$), Renland ($r = 0.38$, $p = 0.05$), GRIP ($r = 0.34$, $p > 0.1$), Agassiz ($r = 0.3$, $p > 0.1$), GISP2 ($r = 0.27$, $p = 0.02$), and Dye-3 ($r = 0.25$, $p = 0.04$) (Table 2). The observations that the GISP2 $\delta^{18}O_{ice}$ has the highest correlation with the Dye-3 $\delta^{18}O_{ice}$ and that the two records exhibit relatively low correlation with the temperature may indicate that the GISP2 and Dye-3 $\delta^{18}O_{ice}$ were affected by similar regional climatic patterns, such as changes in storm tracks and seasonal accumulation, as both located in the south western slope of the Greenland ice sheet (Ohmura and Reeh, 1991; Rogers et al., 1998).





CPD
8, 4817–4883, 2012

Causes of Greenland temperature variability over the past 4000 yr

T. Kobashi et al.

We conducted principal component analysis on the six $\delta^{18}O_{ice}$ records (Table 3). The first principal component (PC1) of the six $\delta^{18}O_{ice}$ explains 44 % of total variance and is highly correlated with the temperature time series, with a correlation coefficient of $r = -0.49$ ($p = 0.05$) (Table 2; Fig. 7). The correlation coefficient is higher than any of the individual correlations with temperature (Table 2). PC1 exhibits a nearly identical character ($r = -0.99$) to a simple average (stacking) of the six $\delta^{18}O_{ice}$ records, indicating that stacking of the $\delta^{18}O_{ice}$ records reduces noise, as suggested in earlier studies (Fisher et al., 1996; White et al., 1997), and reflecting the fact that Central Greenland is representative of the overall temperature variability in Greenland (Kobashi et al., 2011).

Vinther et al. (2009) developed a Greenland temperature record over the Holocene using Agassiz and Renland $\delta^{18}O_{ice}$ after independently correcting for uplift, assuming that Agassiz and Renland $\delta^{18}O_{ice}$ represent the temperature trend of Greenland (Vinther et al., 2009). Correlation between Greenland temperatures developed by Kobashi et al. (2011) and Vinther et al. (2009) are not significant with $r = 0.41$ ($p = 0.12$), and the correlation coefficient is lower than the correlation between the temperature and PC1 (stacking) ($r = 0.49$). As the reconstructed temperature and elevation changes by Vinther et al. (2009) were based on several assumptions that are likely not valid at least for the past 4000 yr, it is necessary to revisit the link between changes in elevation and $\delta^{18}O_{ice}$ when argon and nitrogen temperature estimates become available from more core sites.

# 4 Solar influence on Greenland climate over the past 4000 yr

## 4.1 Solar influence on Greenland temperature over the past 4000 yr

Greenland is uniquely located in the Northern North Atlantic, where climatic variation is considerably affected by the NAO/AO. Atmospheric dipoles of high and low pressure at the surface are located near the Azores and Iceland, respectively, and fluctuation in pressure differences between the two centers of action induce variations in westerlies





CPD
8, 4817–4883, 2012

in the North Atlantic and northerly winds in Greenland (Hurrell, 1995; Hurrell et al., 2003; Wanner et al., 2001). Therefore, Greenland experiences cooling when Northern Europe experiences warming (positive NAO), and vice versa (Hurrell, 1995). Climate models and observations have indicated that solar variability induces changes in atmospheric circulation, such as the NAO/AO, though ozone feedback in the stratosphere (Shindell et al., 2001; Gray et al., 2010; Kodera and Kuroda, 2002). When solar activity is stronger (weaker), changes in the positive (negative) NAO/AO-like atmospheric circulation are induced, such that Greenland temperatures are cooler (warmer) compared to NH average temperatures (Kobashi et al., 2012; Shindell et al., 2001; Hurrell, 1996; Lean and Rind, 2008). In addition, other mechanisms (Renssen et al., 2006) have been proposed to explain the negative responses of Greenland temperatures to solar variability. A climate model indicated that during weaker (stronger) solar activity, formation of deep water in the Nordic seas relocates to (from) near Iceland because of increased (decreased) sea ice in the Nordic seas, which warms (cools) Southeast Greenland due to the large heat release in the convective areas (Renssen et al., 2006).

Changes in past solar activity can be estimated from the variation in cosmogenic nuclides, such as $^{14}$C in tree-rings (Vieira et al., 2011) and/or $^{10}$Be concentration in ice cores (Fig. 8) (Steinhilber et al., 2009). The estimation of these changes is possible because during periods of stronger (weaker) solar activity, the intensity of the galactic cosmic rays that produce cosmogenic nuclides such as $^{10}$Be and $^{14}$C from nitrogen and oxygen is reduced (increased) due to stronger (weaker) solar magnetic fields (Gray et al., 2010; Lal and Peters, 1968). As both $^{10}$Be- and $^{14}$C-based estimates have different advantages and disadvantages owing to different chemical characters (Usoskin et al., 2009), a recent reconstruction of total solar irradiance (TSI) (Steinhilber et al., 2012) utilized all available $^{10}$Be (from Greenland and Antarctic ice cores) and $^{14}$C data to produce "combined" estimates of TSI. Three TSI estimates from "$^{14}$C-based" (Vieira et al., 2011), "$^{10}$Be-based" (from Greenland ice cores) (Steinhilber et al., 2009), and "combined" methods (Steinhilber et al., 2012) exhibit a similar trend over the past 4000 yr (Fig. 8), but the combined estimate exhibits the least multi-decadal variation as it





CPD
8, 4817–4883, 2012

captures only common variance in $^{14}$C and $^{10}$Be that which likely provide the most robust estimate of past solar activity (Steinhilber et al., 2012). We note that the correlation between the "combined" and "$^{14}$C-based" estimates is higher ($r = 0.87$, $p < 0.01$) than that ($r = 0.67$, $p < 0.01$) between the "combined" and "$^{10}$Be-based" estimates, likely because the local climate (e.g. high accumulation rate) in Greenland affected $^{10}$Be deposition. Therefore, we primarily used the combined TSI estimates (Steinhilber et al., 2012) for the following analyses and explored uncertainties using $^{14}$C- and $^{10}$Be-based estimates.

The negative responses of Greenland temperatures to solar variability can be observed more clearly if we compare them to NH average temperatures (Kobashi et al., 2012). The Greenland temperature anomaly (GTA) from the NH temperature trend can be calculated by subtracting standardized NH temperatures from standardized Greenland temperatures. Over the past 800 yr, the GTA exhibited significant solar influence (Kobashi et al., 2012). When solar activity is stronger (weaker), Greenland temperatures exhibit negative (positive) deviations from the NH temperature trend. Over the past 4000 yr, Greenland temperatures exhibited a weak positive correlation ($r = 0.10$, $p > 0.1$) with the TSI (Steinhilber et al., 2012) owing to decreasing trends in both datasets. However, after linear detrending of the temperature and TSI data, Greenland temperatures and TSI show a weak negative correlation ($r = -0.08$, $p > 0.1$). As the GTA exhibits multi-decadal to centennial-scale variation from the NH temperature trend, we de-trended the TSI and Greenland temperatures using a high-pass loess filter (a locally weighted least-squares quadratic estimate; Cleveland and Devlin, 1988), removing signals longer than 1150 yr. It was found that multi-decadal to centennial variation in Greenland temperatures (120 RMs) was significantly negatively correlated with the TSI ($r = -0.25$, $p = 0.1$; Fig. 9) over the past 4000 yr, indicating that solar modulation on Greenland temperatures found in the past 800 yr (Kobashi et al., 2012) continued at least over the past 4000 yr.





CPD
8, 4817–4883, 2012

### 4.2 Solar influence on $\delta^{18}O_{ice}$ revisited

Solar influence on oxygen isotopes ($\delta^{18}O_{ice}$) from the GISP2 ice core was investigated by Mints Stuiver more than a decade ago (Stuiver et al., 1995, 1997). Now that the new Greenland temperatures (Kobashi et al., 2011) and more $\delta^{18}O_{ice}$ data from other ice cores are available, we re-visited the issue to explore if there is significant evidence of solar influence on $\delta^{18}O_{ice}$ of six Greenland ice cores over the past 4000 yr. In a previous study (Stuiver et al., 1997), it was found that GISP2 $\delta^{18}O_{ice}$ was significantly positively correlated with $^{14}C$ (solar variability) over the past millennium, but not for the rest of the Holocene. Over the past 4000 yr GISP2 $\delta^{18}O_{ice}$ does not exhibit a significant correlation with TSI data, but the Dye-3 and Renland $\delta^{18}O_{ice}$ records, both of which are southern and eastern coastal high accumulation sites (Fig. 2), do exhibit significant positive correlations of $r = 0.28$ ($p = 0.03$) and $r = 0.34$ ($p = 0.03$), respectively (Table 2). NGRIP $\delta^{18}O_{ice}$, which has the highest correlation with the temperature, is little correlated with the TSI. We note that PC1 has a significant positive correlation ($r = 0.37$, $p = 0.1$) with the TSI (Table 2).

Earlier studies (Vinther et al., 2003; White et al., 1997; Barlow et al., 1997) found that $\delta^{18}O_{ice}$ in winter months in Southern to Central Greenland was negatively correlated with the winter NAO index, because local temperatures negatively correlated with the winter NAO index on the annual to inter-decadal time scale. As discussed earlier, multi-decadal to centennial variation of Greenland temperatures negatively correlated with the TSI over the past 4000 yr. Therefore, the observed positive correlations of $\delta^{18}O_{ice}$ with the TSI on the multi-decadal to centennial time scale over the past 4000 yr, especially for the two coastal sites, must be explained by processes other than local temperature changes. There are two possible explanations. First, Greenland accumulation rates, especially in Western Greenland, have negative correlations with the NAO index (Appenzeller et al., 1998a, b). It is possible that during the positive (negative) NAO, caused by stronger (weaker) solar activity, reduced (increased) accumulation in



CPD
8, 4817–4883, 2012

Causes of Greenland temperature variability over the past 4000 yr

T. Kobashi et al.

winter may have shifted the average annual $\delta^{18}O_{ice}$ signals toward summer (winter), resulting in the apparent positive correlation of $\delta^{18}O_{ice}$ with solar variability.

Another possibility is related to vapor source temperature and wind direction. During the solar-induced positive (negative) NAO, vapor source areas, where storm-related precipitation originates, experience cooling (warming) with stronger (weaker) northerly winds, which create smaller (larger) temperature gradients between vapor-source and snow-fall sites in Greenland (White et al., 1997). Therefore, water vapor experiences less (more) isotopic fractionation during transport such that precipitation in Greenland has heavier (lighter) $\delta^{18}O_{ice}$ with an apparent positive correlation with the NAO index. These processes must be balanced with the influence of local temperatures, which exhibit negative correlations with the NAO index. We also note that a fair amount of vapor is transported from low latitudes to Greenland (Werner et al., 2001). There is strong evidence that monsoon activity has been strongly controlled by changing solar outputs (Neff et al., 2001; Wang et al., 2005a; Fleitmann et al., 2003). It is plausible that positive solar signals are transported from these regions to South and East Greenland with high accumulation.

The weights of various influences on $\delta^{18}O_{ice}$ may be different depending on the time scale. To determine the precise mechanisms and balance among the various processes, it is necessary to use atmosphere ocean-coupled general circulation models (AOGCMs) solving for solar-induced atmospheric and oceanic changes (e.g. stratospheric ozone feedbacks) and tagging water vapor in the hydrological cycle with isotopes. A correct understanding of these processes will aid in the projection of more accurate future changes to the Greenland ice sheet.

## 5 Climate change of the Late Holocene: perspective from Greenland temperature over the past 4000 yr

How much the current and future climate that is induced by human activity differs from the past is an important question for understanding human societal and ecological





CPD
8, 4817–4883, 2012

resilience to climate change. Therefore, global to hemispheric average temperatures over the past few millennia have been reconstructed using various types of temperature proxies and methods (Jones and Mann, 2004; Mann et al., 1999, 2008; Moberg et al., 2005; Ljungqvist et al., 2012; Christiansen and Ljungqvist, 2011; Hegerl et al., 2007). The results have shown that the present decadal NH average temperatures are likely higher than anytime during the past 2000 yr (Mann et al., 2008; Moberg et al., 2005). With the progression further back in time, uncertainties in temperature proxies and dating increase, such that the compilation of proxy temperatures to derive global to hemispheric average temperatures becomes difficult. Therefore, we attempted to infer the north hemispheric temperature trend over the past 4000 yr from the physically constrained Greenland temperatures (Kobashi et al., 2011), of which regional temperature patterns from the NH trend are well understood (Kobashi et al., 2012). To better understand the mechanisms of temperature change over the past 4000 yr, we also employed a one-dimensional energy balance model (1d-EBM) with reconstructed climate forcings over the past 4000 yr.

### 5.1 Climate forcings over the past 4000 yr

Climate change over the past 4000 yr was primarily caused by variations in orbital, solar, volcanic, and greenhouse gas forcing (Wanner et al., 2008). Because the residual Laurentide ice-sheet from the last glacial period nearly disappeared by approximately 6000 yr Before Present (BP; Present is defined as 1950), climate boundary conditions (e.g. sea level and areas covered by ice sheets) over the past 4000 yr were largely the same as those of the preindustrial period (Wanner et al., 2008; Kaufman et al., 2004; Lambeck and Chappell, 2001). Over the past 1000 yr, natural variability in the average NH temperature can be explained predominantly by changes in solar irradiance and volcanism (Ammann et al., 2007; Crowley, 2000). For the past 4000 yr, orbital forcing becomes non-negligible, as discussed later, especially for high latitude regions. We investigated if the relationship between climate forcings and climate over the past 1000 yr can be applied to the past 4000 yr, constrained by the Greenland temperature.

A better understanding of the past 4000 yr of temperature change provides an important test case to understand climate variability at the multidecadal to centennial time scale, which is highly relevant to social affairs.

#### 5.1.1 Orbital forcing

As Greenland is located in the high latitudes of the NH, seasonal variation of insolation is a large event at present and it has varied with a comparatively large magnitude over the past 4000 yr, largely owing to changes in Earth's axial tilt (obliquity) (Laskar et al., 2004) (Fig. 10). Mean annual insolation at the Greenland Summit decreased by 1.4 % from 195.4 $W m^{-2}$ in 2000 B.C.E. to 192.8 $W m^{-2}$ in 2000 C.E. (Fig. 10). At present, annual mean insolation is still decreasing at a rate of 0.44 $W m^{-2}$ per 100 yr in Greenland (Laskar et al., 2004). As Greenland has no sun light during the winter, most of the insolation change occurred in the summer (Fig. 10) (Laskar et al., 2004). In contrast, global mean annual insolation through orbital configuration has been nearly constant over the past 4000 yr, indicating that differential changes in insolation at different latitudes compensated for each other (Laskar et al., 2004). The decrease at high latitude insolation contrasts with that at low latitudes over the past 4000 yr, which exhibited a slight increase over the past 4000 yr (Fig. 11). It is noted that July insolation decreased over the entire NH over the past 4000 yr, but the decrease was compensated by an increase in winter insolation in the case of low latitudes.

#### 5.1.2 Solar forcing

During the last 4000 yr, total solar irradiance exhibited variability in a range (maximum – minimum) of 1.23 $W m^{-2}$ or approximately 0.1 % and had a slight decreasing trend of approximately 0.1 $W m^{-2}$ per 1000 yr (Steinhilber et al., 2012) (Fig. 8). There are several periods (approximately 1500, 800, 400 B.C.E. and 600, 1000, 1300, 1500, 1600, 1850 C.E.) of weaker solar activity similar to the Maunder Minimum, some of which reportedly caused cooling events in wide spread areas (Mayewski et al., 2004;





CPD
8, 4817–4883, 2012

Wanner et al., 2008, 2011). The Little Ice Age and the 2.8 ka event are well-known cooling periods of the past 4000 yr (Wanner et al., 2008; Renssen et al., 2006). The standard deviation of radiative forcing ($\Delta F$) by TSI variation from 2000 B.C.E. to 1750 C.E. is calculated to be 0.07 ($\mathrm{W\,m^{-2}}$) from the following equation: $\Delta F = \Delta \mathrm{TSI}/4 \times 0.7$ (Forster et al., 2007). We note that for the 1d-EBM calculation average values of albedo in each latitudinal band were applied to calculate solar forcing.

### 5.1.3 Greenhouse gas forcing

Important long-lived greenhouse gasses in the atmosphere are $CO_2$, $CH_4$, and $N_2O$ (Forster et al., 2007). Although concentrations of these gasses in the atmosphere have been rapidly increasing due to human activity since industrialization (~ 1850 C.E.), they can also vary naturally, but with much smaller amplitudes (Forster et al., 2007). Past variation in these gasses can be obtained from ice cores (Fig. 12). We used the data for the past 2000 yr compiled by F. Joos for PMIP3 (Schmidt et al., 2011) (https://pmip3.lsce.ipsl.fr/wiki/doku.php/pmip3:design:lm:final). For older periods, lower resolution data were used for $CO_2$ (Monnin et al., 2004), $CH_4$ (averages of Siple Dome and GISP2 data) (Brook, 2009), and $N_2O$ (Flückiger et al., 2002). Slight adjustments were made to avoid gaps between C.E. and B.C.E. by subtracting the differences in average concentrations in the overlapping period from 1–12 C.E. from the values used for B.C.E. The concentration data were calibrated to radiative forcing, $\Delta F$ ($\mathrm{W\,m^{-2}}$) according to the following equations (Ramaswamy et al., 2001). For $CO_2$, $\Delta F = \alpha \ln(C/C_0)$, where $\alpha$ is 5.35, and C is $CO_2$ in ppm. For $CH_4$, $\Delta F = \alpha(\sqrt{M} - \sqrt{M_0}) - (f(M,N_0) - f(M_0,N_0))$, where $\alpha$ is 0.036 and $M$ is $CH_4$ in ppb. For $N_2O$, $\Delta F = \alpha(\sqrt{N} - \sqrt{N_0}) - (f(M_0,N) - f(M_0,N_0))$, where $\alpha$ is 0.12 and N is $N_2O$ in ppb. A function "$f$" is described as $f(M,N) = 0.47 \ln[1 + 2.01 \times 10^{-5}(MN)^{0.75} + 5.31 \times 10^{-15} M(MN)^{1.52}]$. The subscript 0 denotes the concentrations in the year 1750. Standard deviations of $\Delta F$ for $CO_2$, $CH_4$, and $N_2O$ for the period from 2000 B.C.E to 1750 C.E. are 0.06 ($\mathrm{W\,m^{-2}}$), 0.02 ($\mathrm{W\,m^{-2}}$), and 0.01 ($\mathrm{W\,m^{-2}}$), indicating that $CO_2$ variation





CPD
8, 4817–4883, 2012

had the largest control on temperature changes among the greenhouse gases during this period. The standard deviation of total $\Delta F$ from the three greenhouse gasses from 2000 B.C.E. to 1750 C.E. is 0.08 ($\mathrm{W\,m^{-2}}$). There is a slight increasing trend in total greenhouse gas forcing, $\Delta F$ of 0.1 $\mathrm{W\,m^{-2}}$ per 1000 yr from 2000 B.C.E to 1750 C.E. (Fig. 13). In addition, we included aerosol forcing from 1892 C.E. onward (Crowley, 2000) (Fig. 13).

#### 5.1.4 Volcanic forcing

Large volcanic eruptions are known to cause climate change by injecting chemically and microphysically active gases and aerosols into the atmosphere, which affect Earth's radiative balance (Robock, 2000). Sulfate data in ice cores provide the best record of past volcanic events; as a result, there have been many attempts to estimate stratospheric sulphate loading and optical depth (Zielinski et al., 1994; Zielinski, 1995; Cole-Dai et al., 2000; Gao et al., 2008). We used the GISP2 sulfate record for reconstructions of volcanic forcing as it is the only currently available record that has high resolution and a good chronology with continuous bi-annual resolution (averages of two years) over the past 4000 yr (Zielinski et al., 1994; Mayewski et al., 1997). Multi-core analysis indicated that volcanic debris was fairly evenly distributed in the atmosphere after volcanic eruptions (Gao et al., 2007), which is an important factor in inferring the magnitudes of past volcanic eruptions from a single ice core.

The GISP2 sulfate record has been used to estimate volcanic events over the past 9000 yr (Zielinski et al., 1994), as well as stratospheric loading and optical depth from volcanic eruptions over the past 2100 yr (Zielinski, 1995). More recently, using multiple cores from both the polar regions of Greenland and Antarctic, volcanic events and their associated stratospheric loading over the past 1500 yr were reconstructed (Gao et al., 2008). Although multi-core estimation is clearly more reliable, we attempted a single core reconstruction with GISP2 due to the lack of multi-core estimation for the entire period, and evaluated the results with multi-core estimates for an overlapping period. One caveat is that a single-core-reconstruction cannot differentiate latitudinal variations in sulfate loading, as sulfate loading from volcanic eruptions near Greenland (e.g. Iceland) is inevitably larger. This is presumably less problematic when a single-core-reconstruction is used as volcanic forcing for northern high-latitudes, but care must be taken to interpret it as a hemispheric scale forcing.

To estimate stratospheric loading over the past 4000 yr, we extracted volcanic signals from the sulfate ion record of the GISP2 ice core (Mayewski et al., 1997), largely following the methodology developed by Gao et al. (2006, 2007, 2008). To be consistent with the time scale of the temperature reconstruction (Kobashi et al., 2008b, 2011), we applied a GISP2 time scale, called "visual stratigraphy" (Alley et al., 1997), to the GISP2 sulfate record. Therefore, age uncertainties between the temperature and reconstructed volcanic forcing are at a minimum, which is important as the climatic impacts of volcanic eruptions last for only a few years (Robock, 2000). It is noted that the GISP2 sulfate record is reliable, as it matches quite well with other Greenland core data (unpublished data).

First, sulfate ion data (ppb) (Mayewski et al., 1997) from the GISP2 ice core were converted to sulfate flux using accumulation rate data (Alley et al., 1997). Then, a high-pass loess filter (Cleveland and Devlin, 1988) was applied to remove signals longer than 31 yr (Gao et al., 2008). We only extracted signals larger than the running median absolute deviation (RMAD) multiplied by 0.5. We chose 0.5 instead of 2, as in the original methodology by Gao et al. (2008), to extract slightly more volcanic events over the past 1500 yr, because peaks from a single core may miss some of the important volcanic signals detected in multi-core analysis. Although it is still possible to miss relatively minor volcanic signals or to identify incorrect signals, our results should not be affected because these signals are small and thus climatically less significant. With this procedure, 72 peaks were extracted from the GISP2 sulfate record, compared to 63 peaks in Gao et al. (2008), for NH volcanic events for the past 1500 yr.

To calibrate the selected GISP2 volcanic signals to stratospheric volcanic sulfate aerosol loading ($T$), we summed the volcanic signals from GISP2 over the past 1500 yr and then scaled it to the sum of the stratospheric volcanic sulfate aerosol loading ($T$) for



Discussion Paper | Discussion Paper | Discussion Paper | Discussion Paper |

CPD

8, 4817–4883, 2012

Causes of Greenland temperature variability over the past 4000 yr

T. Kobashi et al.

the NH by Gao et al. (2008). Then, the scaling factor was used to reconstruct the entire volcanic record over the past 4000 yr. It is assumed that sulfate life time in the stratosphere has an e-holding time of 1 yr (Crowley, 2000). As we were investigating the impacts of volcanic events on multi-decadal to centennial temperature changes, a 51 yr running mean (RM) filter was applied to the time series. The reconstructed stratospheric volcanic sulfate aerosol loading data from the single-core and multiple cores agree well, with a correlation coefficient of $r = 0.68$ over the past 1500 yr (Fig. 14), indicating that a single core estimate can reconstruct NH volcanic forcing sufficiently well. Climate forcing ($\Delta F$) of the calculated stratospheric volcanic sulfate aerosol loading was derived by converting the sulfate loading to aerosol optical depth (AOD = aerosol loadings/150$T$; Stothers, 1984). Then, the AOD was multiplied by $-20\,\mathrm{W\,m^{-2}}$ to obtain $\Delta F$ (Wigley et al., 2005). The standard deviation (51 yr RMs) of the volcanic forcing over the period from 2000 B.C.E to 1750 C.E. is $0.15\,\mathrm{W\,m^{-2}}$, which is approximately 2 times larger than the standard deviations of greenhouse-gas and solar forcings over the same period (Fig. 13).

Over the past 4000 yr, we identified 17 volcanically active periods (Fig. 15 and Table 4), and it is clear that volcanic events were most frequent during the Little Ice Age. In the NH, eight volcanically active periods can be identified during the first two millennial B.C.E., during which one or several large volcanic events had impacts on the climate (Fig. 15, Table 4, see later discussion). In contrast, Southern Hemisphere records exhibit very few volcanic events during the first two millennia B.C.E. (Cole-Dai et al., 2000; Wanner et al., 2008). In terms of volcanic events, 0–600 C.E. was a rather calm period (Fig. 15). The largest volcanic event during the past 4000 yr occurred at 1258–1259 C.E. Climate responses are somewhat ambiguous for this event as tree-rings (Mann et al., 2012) and $\delta^{18}O_{ice}$ in Greenland (Zielinski, 1995) did not show clear signals of climate change, perhaps owing to the character of proxy (Mann et al., 2012) or lower climate sensitivity to volcanic events during the warmer Medieval Warm Period (Zielinski, 1995).





CPD
8, 4817–4883, 2012

### 5.1.5 Integrating climate forcings and calculating temperature changes in different latitudinal bands using 1d-EBM

As five climate forcings (orbital, solar, volcanic, greenhouse gases, and aerosols) were quantified as $\Delta F$ from 2000 B.C.E. to 1950 C.E., it is possible to integrate them and calculate the corresponding surface temperatures using climate models. Total forcing, excluding orbital forcing, shows a slight increasing trend from 2000 B.C.E. to approximately 200 C.E., due to increasing greenhouse gas forcing and fewer volcanic eruptions (Fig. 13), and remains relatively high during the first millennium C.E. Then, total forcing decreases, owing to more volcanic eruptions and weaker solar activity toward 1850 C.E. Finally, largely owing to increasing human-induced greenhouse gases, total forcing increases rapidly to the highest level in the past 4000 yr (Fig. 13). According to the calculated forcings, the multi-decadal to centennial variations were caused primarily by volcanic forcing and secondarily by solar and greenhouse forcing during the pre-industrial period (Fig. 13).

To investigate the impacts of orbital forcing at different latitudes, we utilized a one-dimensional energy balance model (1d-EBM; Budyko-Sellers model) (Budyko, 1969; Sellers, 1969) that can be resolved for 18-latitudinal bands ($10^{\circ}$ for each band) over the globe (McGuffie and Henderson-Sellers, 2005). The heat transports into and out of the bands were calculated from the deviations of zonal mean temperatures from global mean temperatures. Observed average albedo for each latitudinal band was used to calculate the energy balance at the latitudinal bands, which were set to be constant through time. EBMs are computationally efficient and calculate mean annual hemispheric temperatures close to the observations (Crowley, 2000; Mann et al., 2012). The 1-d EBM was tested for seasonal heat transport divergence and found to match observations, especially for high latitude regions (Warren and Schneider, 1979).

Latitudinally variable solar insolation (for example, annual insolation at $65^{\circ}$ N was used for a latitudinal band of $60^{\circ}$ N–$70^{\circ}$ N.) was obtained from Laskar et al. (2004). Then, fractions of solar insolation from the present value for each latitudinal band were





CPD
8, 4817–4883, 2012



Title Page
Abstract | Introduction
Conclusions | References
Tables | Figures
◂◂ | ▸▸
◂ | ▸
Back | Close
Full Screen / Esc
Printer-friendly Version
Interactive Discussion

calculated for every year, and applied to all latitudinal bands for each time step (1-yr). Although better forcing estimates are available toward the more recent past, we used the climate forcings described above for the entire period to verify the fidelity of the forcing estimates by comparing them with available temperature records. The model simulation starts at 2200 B.C.E. and calculates until 1950 C.E. Calculated temperatures for a latitudinal band of 70–80° N exhibited a secular decreasing trend over the past 4000 yr owing to orbital forcing, and it contrasts with calculated NH average temperatures that exhibit a similar trend ($r = 0.97$, $p < 0.01$) with that of the total forcings excluding orbital forcing, (Fig. 16, top). This indicates that the influence of orbital forcing on NH annual average temperatures is limited over the past 4000 yr, which is consistent with equilibrium runs for the mid-Holocene (Braconnot et al., 2007) and transient runs (Renssen et al., 2006) of GCM simulations. The model-derived 70–80° N temperatures exhibit warmer temperatures than the ice-core-derived Greenland temperatures because the ice core site is located at high altitude (3200 m a.s.l.). However, average temperatures of the model-derived 70–80° N temperatures (Fig. 16, bottom) are similar to the mean annual temperature ($-11.1 \pm 2.3$ °C) of the northwest coast of Greenland (Pituffik/Thule Air Base; 76° 32′ N, 68° 45′ S) (Box, 2002).

### 5.2 Causes of Greenland temperature variability over the past 4000 yr

Multi-decadal to centennial Greenland temperature anomalies (GTA) from the NH temperature trend were found to be influenced by changes in solar induced NAO/AO-like atmospheric circulation, possibly involving changes in the AMOC over the past 800 yr (Kobashi et al., 2012). During stronger (weaker) solar activity, Greenland temperatures exhibit positive (negative) deviation from the NH temperature trend (Kobashi et al., 2012). The relationship can be written as follows:

$$\begin{aligned}\text{GTA} &= \text{Standardized Greenland temperature} - \text{standardized NH temperature} \\ &= -k(-\text{detrended standardized TSI})\end{aligned} \tag{1}$$



Discussion Paper | Discussion Paper | Discussion Paper | Discussion Paper |

CPD

8, 4817–4883, 2012

where $k$ indicates a scaling coefficient. As no realistic NH average temperatures are available over the past 4000 yr, we calculated the GTA using model estimates of NH temperatures (note that we used 70–80° N temperatures instead of NH temperatures (Fig. 15 top) to account for orbital forcing). As during the past 800 yr, the GTA over the past 4000 yr was significantly influenced by solar variability (a correlation coefficient between the GTA and detrended TSI is $r = -0.41$, $p < 0.01$ as in Fig. 16, middle). We note that the calculated NH temperature contains solar signals as a forcing, such that the GTA and TSI are not totally independent. Therefore, we calculated a north hemispheric temperature history without solar forcing but including all other forcings (as solar forcing exhibits a relatively small contribution to total forcing; see Fig. 13) and then computed the GTA. We found that the GTA was still significantly correlated ($r = -0.21$, $p = 0.05$) with the detrended TSI, noting that they are two totally independent time series (Fig. 16, middle). This indicates the critical role of a negative solar influence and volcanic forcing (the most important forcing for multi-decadal to centennial time scale; see Fig. 13.) on the Greenland temperatures over the past 4000 yr.

From the relationship in the Eq. (1), we calculated a history of Greenland temperatures from the model outputs of 70–80° N average temperatures (Fig. 16, top, red line) by adding a negative solar signal. The scaling coefficient $k$ was obtained as a standard deviation (1.21) of the aforementioned GTA over the past 4000 yr (Fig. 16, middle, red line). The calculated Greenland temperatures are significantly correlated with the ice core-derived Greenland temperatures with a 97 % confidence level ($r = 0.32$, $p = 0.03$; Fig. 17), indicating that the calculated forcing and negative solar singles can explain at least 10 % of the variance in Greenland temperature over the past 4000 yr. Negative solar signals with ($^{14}C$-based and $^{10}Be$-based) TSI data produced Greenland temperatures that have similar significant correlations of $r = 0.27$ ($p = 0.05$) and $r = 0.35$ ($p = 0.03$) with the ice core-derived Greenland temperatures, respectively, confirming the robustness of the result. As the calculated and ice core-derived Greenland temperatures of the past 4000 yr are totally independent, the correlation is not an artifact. Considering the large expected internal variability of the regional climate, this is rather





CPD
8, 4817–4883, 2012

remarkable. A millennial cooling from approximately 500 B.C.E. to 0 C.E. that was observed in the Greenland temperature reconstructions from borehole temperature profiles (Dahl-Jensen et al., 1998) was also found in the calculated temperatures (Fig. 17), indicating that the cooling was caused by several volcanic eruptions and negative responses of Greenland temperatures to solar variability.

### 5.3 Implications for northern high latitude temperature changes over the past 4000 yr

The northern high latitude (NHL) temperature was derived from the ice-core-derived Greenland temperatures and solar signals (combined) following Eq. (1) (Fig. 18). The NHL temperature was extended by 21 yr by adding the Greenland Summit temperatures (Box et al., 2009; Kobashi et al., 2011) from 1994 to 1998 C.E. and adding a TSI record in 21 RMs (Wang et al., 2005b) from 1978 to 1998 for TSI. The three NHL temperatures derived from different TSI estimates generally agree well (Fig. 18, middle), but the correlation ($r = 0.91$, $p < 0.01$) between the "combined" and "$^{14}C$-based" NHL temperatures is higher than the correlation ($r = 0.79$, $p < 0.01$) between the "combined" and "$^{10}Be$-based" NHL temperatures, as mentioned earlier. The "$^{10}Be$-based" NHL temperatures are slightly higher than the other estimates (Fig. 18, middle).

The modeled 70–80° N average temperatures and NHL temperatures are significantly correlated ($r = 0.53$, $p < 0.01$) at the 99 % confidence level over the past 4000 yr (Fig. 16, bottom). The ice core-derived Greenland temperatures and the modeled 70–80° N average temperatures did not exhibit a significant correlation, indicating that the added negative solar signal on the Greenland temperatures is a critical element for the NHL temperatures. As the two time series are not completely independent, because both estimates possess the same TSI signals, we tested the relationship by calculating a modeled 70–80° N average temperature without solar forcing as we did for the GTA. It was found that the model-derived 70–80° N temperature without solar forcing was significantly correlated ($r = 0.33$, $p = 0.03$) with the NHL temperature, noting that now the two time series are totally independent (Fig. 16 bottom). This is unambiguous





CPD
8, 4817–4883, 2012

evidence of the significant influence of large volcanic eruptions on the multidecadal to centennial variation in climate over the past 4000 yr. Most of the important volcanically active periods (Table 4) seem to coincide with large cooling events, such as that at approximately 1700 B.C.E., the 2.8 ka event, and the Little Ice Age (Fig. 16).

Next, we compared the NHL temperature with the extra-tropical Northern Hemisphere mean temperature (30–90° N) (Christiansen and Ljungqvist, 2012) and the polar region temperature (60–90° N; primary summer temperature) (Kaufman et al., 2009) for the overlapping period of the past 2000 yr (Fig. 18). As proxy temperatures generally record spring to summer temperatures (Kaufman et al., 2004, 2009), this provides an opportunity to compare them with an annual average estimate of the NHL temperature. Correlations between the NHL temperature and the polar region temperature and between the NHL temperature and the extra-tropical temperature are remarkably high, with values of $r = 0.60$ ($p = 0.01$) and $r = 0.45$ ($p = 0.06$), respectively, for the past 2000 yr (as shown in Fig. 18, bottom). Therefore, the NHL temperature captures the high latitude temperature trend well. We note that correlations between the ice core-derived Greenland temperatures and extra-tropic or polar-region temperatures are lower ($r = 0.33$, $p = 0.11$ and $r = 0.29$, $p = 0.21$, respectively), supporting negative responses of Greenland temperatures to solar variability. Model outputs of 70–80° N average temperatures (Fig. 16, top) exhibited significant correlations ($r = 0.57$, $p = 0.02$; $r = 0.62$, $p = 0.02$, respectively) with the extra-tropic (Christiansen and Ljungqvist, 2012) and polar average temperatures (Kaufman et al., 2009) in 21RMs over the past 2000 yr, indicating that 18–38 % of the variance in the temperatures can be explained by the reconstructed climate forcings.

Figure 19 shows the NHL and polar region (Kaufman et al., 2009) temperatures and the modelled 70–80° N average temperatures with all forcings and without greenhouse gas forcing. From the two model outputs, it can be concluded that greenhouse gas forcing played two critical roles over the past 4000 yr. One is that it caused cooler temperatures in earlier periods than temperatures without greenhouse gas forcing (owing to a long-term increase in greenhouse gas forcing), and importantly, the other is that it caused a rapid warming during the 20th century (Fig. 19). Departure between the NHL (and polar region) temperature and the modeled 70–80° N average temperature without greenhouse gas forcing stared at approximately 1900 C.E (Fig. 13), and it is clear that no large warming would have occurred during the 20th century without greenhouse gas forcing. This reinforces earlier findings (Solomon et al., 2007) that an increase in the NHL (polar region) temperature during the 20th century cannot be explained without human-induced greenhouse gas increases. In addition, extending the conclusion of Kaufman et al. (2009) for the past 2000 yr, the late 20th century average temperature in the northern high latitude is likely warmer than at any time during the past 4000 yr (Fig. 19).

### 5.4 Implications for NH average temperature changes over the past 4000 yr

The model outputs indicate that 70–80° N and NH average temperature responses to climate forcings are different only in their long-term trends (Fig. 16, top). Over the past 4000 yr, low latitudes experienced increasing mean annual insolation and high latitudes experienced decreasing mean insolation (Fig. 11). As low latitudes have larger areas than high latitudes, NH average temperature generally follows low latitude temperature trends under conditions of a constant background climate. Keeping this in mind, we compared the NHL temperatures with two NH average proxy temperature records (Fig. 20). To assign a temperature scale to the NHL index, it was standardized and scaled to the average standard deviation of Moberg et al. (2005) and Mann et al. (NHHAD_EIV) (Mann et al., 2008) proxy NH temperatures in 21 RMs for the past 1000 yr. The absolute values were assigned by comparing the temperature scale with an average of observed NH average temperatures (21 RMs) from the period from 1860 to 1977 (HadCUT3; Brohan et al., 2006) (Fig. 20).

The NHL temperature generally agrees with the observed and proxy NH temperatures for the overlapping periods (Fig. 20). Correlations between Moberg et al. NH temperatures are $r = 0.34$ ($p = 0.14$) and $r = 0.52$ ($p = 0.08$) for periods from 11 C.E to 1969 C.E. and 1200C.E. to 1969 C.E. Correlations between Mann et al. (2008) NH





CPD
8, 4817–4883, 2012

temperatures are $r = 0.44$ ($p = 0.10$) and $r = 0.51$ ($p = 0.05$) for periods from 11 C.E. to 1969 C.E. and 1200 C.E. to 1969 C.E., respectively. Therefore, both of the NH proxy temperature records are at least significantly correlated with the NHL temperatures over the past 800 yr (Fig. 20). The poorer correlations in the longer periods may reflect the effects of latitudinally variable mean insolation for the period or may be due to the poor quality of the NH proxy temperature, as the two proxy NH temperature estimates diverged in the earlier period of the past 2000 yr. Considering the fact that northern high latitude average temperatures are affected by decreasing annual insolation, owing to orbital forcing over the past 4000 yr (Fig. 16), NH average temperatures should have a smaller decreasing temperature trend than the NHL temperature trend over the past 4000 yr (Fig. 20). Therefore, as the current decadal temperature of the NHL is higher than at any time over the past 4000 yr, it is likely that the current decadal NH average temperature is higher than at any time over the past 4000 yr (Fig. 20).

Based on the 4000 yr long NH temperature estimate, we found that the magnitudes of the two sequential cooling events at approximately 800 and 400 B.C.E. (the 2.8 ka event) were similar to the Little Ice Age, although the duration was shorter. The 2.8 ka event has been thought to be global (Chambers et al., 2007), and reportedly caused by decreasing solar outputs (Chambers et al., 2007; Martin-Puertas et al., 2012). However, we found that large volcanic events played equally important roles in cooling (Fig. 13). The 2.8 ka event corresponds to the Iron Age Cold Epoch in the Mediterranean-European climatic zone (Fig. 20). The model and observations indicate a warm inflow in the North Icelandic shelf influenced areas near Iceland and East Greenland during the event, contrasting with the wide spread cooling especially around the North Atlantic basin (Renssen et al., 2006). The 2.8 ka event and the Little Ice Age were parts of the Bond cycle that persisted in the North Atlantic with a 1500 yr period (Fig. 18). As the Little Ice Age and the 2.8 ka event can be explained by volcanic and solar forcings, the Bond cycle may well be caused by these forcings (Fig. 18).

Lastly, we compared the NHL temperature with a speleotherm $\delta^{18}O$ record from Dongge cave that reflects changes in Asian monsoon strength (Wang et al., 2005a)

(Fig. 21). The record exhibits a long-term trend similar to a North Hemisphere summer insolation curb (the timing of the insolation minimum is slightly different in the different latitudes from June to July) (Fig. 21 top), which indicates that the Asian summer monsoons closely followed summer insolation changes (Wang et al., 2005a). Detrending the long-term trend, the multidecadal to multi-centennial variation exhibited a significant correlation ($r = -0.29$, $p = 0.01$ in 21RMs) with the NHL temperatures (Fig. 21 bottom), indicating a possible link between the Asian monsoons and north hemispheric temperatures on the multi-decadal to multi-centennial time scale. We note that the detrended Dongge cave record also exhibits a significant correlation with the detrended TSI ($r = -0.33$, $p < 0.01$) (Wang et al., 2005a). During the 2.8 ka and subsequent cooling events, the Asian monsoon failed substantially with significant cooling (Fig. 21). These events may have forced people to migrate from the continent to the warmer and more humid islands of Japan, bringing their continental culture (e.g. irrigation) (Diamond, 1998) and marking the beginning of the Yayoi period in Japan.

## 6 Conclusions

The Greenland temperatures over the past 4000 yr reconstructed from trapped air within the GISP2 ice core (Kobashi et al., 2011) provided an exceptional opportunity to investigate late Holocene climate changes because of several advantages: (1) the resolving of precise multi-decadal to millennial temperature variation; (2) the recording of “mean” annual temperatures (many paleo-temperatures are spring to summer proxies); (3) the tight age control; (4) the understanding of regional climate (Kobashi et al., 2012); and (5) the plentiful paleoclimate information that is available from the GISP2 ice core. With reconstructed climate forcings (volcanic, solar, orbital, greenhouse gases, and aerosols) over the past 4000 yr, we calculated high latitude temperatures with 1d-EBM and then Greenland temperatures considering negative Greenland temperature responses to changes in solar output. Calculated Greenland temperatures are significantly correlated with ice core-derived Greenland temperatures, indicating that



CPD
8, 4817–4883, 2012

reconstructed climate forcings can explain at least 10 % of Greenland temperature variability over the past 4000 yr. Then, we derived northern high latitude temperatures (NHL temperatures) from the ice core-derived Greenland temperatures. This result indicated that the current decadal average NH temperature is likely warmer than at any time over the past 4000 yr.

This is the first step in utilizing high-quality paleo-temperature data with the possibility of extending its inferences to hemispheric temperature trends. The next step toward a full understanding of the late Holocene climate changes is to evaluate these inferences with careful proxy compilations and the application of Atmospheric Ocean–General Circulation Models.

*Acknowledgements.* We appreciate useful discussions with D. T. Shindell, K. Kodera, and K. Horiuchi. B. M. Vinther and S. O. Rasmussen kindly provided match points between GICC05 and GISP2. This project is supported by KAKENHI 23710020. The production of this paper was supported by an NIPR publication subsidy.

## References

Alley, R. B. and Koci, B. R.: Recent warming in Central Greenland?, Ann. Glaciol., 14, 6–8, 1990.

Alley, R. B., Shuman, C. A., Meese, D. A., Gow, A. J., Taylor, K. C., Cuffey, K. M., Fitzpatrick, J. J., Grootes, P. M., Zielinski, G. A., Ram, M., Spinelli, G., and Elder, B.: Visual-stratigraphic dating of the GISP2 ice core: basis, reproducibility, and application, J. Geophys. Res.-Oceans, 102, 26367–26381, 1997.

Ammann, C. M., Joos, F., Schimel, D. S., Otto-Bliesner, B. L., and Tomas, R. A.: Solar influence on climate during the past millennium: results from transient simulations with the NCAR Climate System Model, Proc. Natl. Acad. Sci. USA, 104, 3713, doi:10.1073/pnas.0605064103, 2007.

Appenzeller, C., Schwander, J., Sommer, S., and Stocker, T.: The North Atlantic Oscillation and its imprint on precipitation and ice accumulation in Greenland, Geophys. Res. Lett., 25, 1939–1942, 1998a.

Appenzeller, C., Stocker, T., and Anklin, M.: North Atlantic Oscillation dynamics recorded in Greenland ice cores, Science, 282, 446–449, 1998b.

Barlow, L., Rogers, J., Serreze, M., and Barry, R.: Aspects of climate variability in the North Atlantic sector: discussion and relation to the Greenland Ice Sheet Project 2 high-resolution isotopic signal, J. Geophys. Res.-Oceans, 102, 26, doi:10.1029/96JC02401, 1997.

Box, J. E.: Survey of Greenland instrumental temperature records: 1873–2001, Int. J. Climatol., 22, 1829–1847, 2002.

Box, J. E., Yang, L., Bromwich, D. H., and Bai, L. S.: Greenland ice sheet surface air temperature variability: 1840–2007, J. Climate, 22, 4029–4049, 2009.

Braconnot, P., Otto-Bliesner, B., Harrison, S., Joussaume, S., Peterchmitt, J.-Y., Abe-Ouchi, A., Crucifix, M., Driesschaert, E., Fichefet, Th., Hewitt, C. D., Kageyama, M., Kitoh, A., Laîné, A., Loutre, M.-F., Marti, O., Merkel, U., Ramstein, G., Valdes, P., Weber, S. L., Yu, Y., and Zhao, Y.: Results of PMIP2 coupled simulations of the Mid-Holocene and Last Glacial Maximum – Part 1: experiments and large-scale features, Clim. Past, 3, 261–277, doi:10.5194/cp-3-261-2007, 2007.

Brohan, P., Kennedy, J., Harris, I., Tett, S., and Jones, P.: Uncertainty estimates in regional and global observed temperature changes: a new dataset from 1850, J. Geophys. Res, 111, D12106, doi:10.1029/2005JD006548, 2006.

Brook, E. J.: Methane Measurements from the GISP2 and Siple Dome Ice Cores, National Snow and Ice Data Center, Boulder, Colorado, USA, 2009.

Budyko, M. I.: The effect of solar radiation variations on the climate of the earth, Tellus, 21, 611–619, 1969.

Chambers, F. M., Mauquoy, D., Brain, S. A., Blaauw, M., and Daniell, J. R. G.: Globally synchronous climate change 2800 years ago: proxy data from peat in South America, Earth Planet. Sc. Lett., 253, 439–444, 2007.

Charles, C. D., Rind, D., Jouzel, J., Koster, R. D., and Fairbanks, R. G.: Glacial–interglacial changes in moisture sources for greenland – influences on the ice core record of climate, Science, 263, 508–511, 1994.

Christiansen, B. and Ljungqvist, F. C.: Reconstruction of the extra-tropical NH mean temperature over the last millennium with a method that preserves low-frequency variability, J. Climate, 24, 6013–6034, 2011.





CPD
8, 4817–4883, 2012

Christiansen, B. and Ljungqvist, F. C.: The extra-tropical Northern Hemisphere temperature in the last two millennia: reconstructions of low-frequency variability, Clim. Past, 8, 765–786, doi:10.5194/cp-8-765-2012, 2012.
Chylek, P., Folland, C., Frankcombe, L., Dijkstra, H., Lesins, G., and Dubey, M.: Greenland ice core evidence for spatial and temporal variability of the Atlantic Multidecadal Oscillation, Geophys. Res. Lett., 39, L09705, doi:10.1029/2012GL051241, 2012.
Cleveland, W. S. and Devlin, S. J.: Locally weighted regression: an approach to regression analysis by local fitting, J. Am. Stat. Assoc., 83, 596–610, 1988.
Cole-Dai, J., Mosley-Thompson, E., Wight, S. P., and Thompson, L. G.: A 4100-year record of explosive volcanism from an East Antarctica ice core, J. Geophys. Res, 105, 2431–24441, 2000.
Crowley, T. J.: Causes of climate change over the past 1000 years, Science, 289, 270–277, 2000.
Crowley, T. J. and North, G. R.: Paleoclimatology, 18, Oxford University Press, New York, NY, USA, 1996.
Cuffey, K. M. and Clow, G. D.: Temperature, accumulation, and ice sheet elevation in Central Greenland through the last deglacial transition, J. Geophys. Res.-Oceans, 102, 26383–26396, 1997.
Cuffey, K. M., Clow, G. D., Alley, R. B., Stuiver, M., Waddington, E. D., and Saltus, R. W.: Large Arctic temperature-change at the Wisconsin-Holocene glacial transition, Science, 270, 455–458, 1995.
Dahl-Jensen, D., Mosegaard, K., Gundestrup, N., Clow, G. D., Johnsen, S. J., Hansen, A. W., and Balling, N.: Past temperatures directly from the Greenland Ice Sheet, Science, 282, 268–271, 1998.
Dansgaard, W.: Stable isotopes in precipitation, Tellus, 16, 436–468, 1964.
Diamond, J.: Japanese roots, Discover, 19, 86–95, 1998.
Dima, M. and Lohmann, G.: A hemispheric mechanism for the Atlantic multidecadal oscillation, J. Climate, 20, 2706–2719, 2007.
Enfield, D. B., Mestas-Nunez, A. M., and Trimble, P. J.: The Atlantic multidecadal oscillation and its relation to rainfall and river flows in the continental US, Geophys. Res. Lett., 28, 2077–2080, 2001.
Fisher, D. A., Koerner, R. M., Kuivinen, K., Clausen, H. B., Johnsen, S. J., Steffensen, J. P., Gundestrup, N., and Hammer, C. U.: Inter-comparison of ice core $^{18}$O and precipitation records

from sites in Canada and Greenland over the last 3500 years and over the last few centuries in detail using EOF techniques, NATO ASI series I, Global Environ. Change, 41, 297–330, 1996.

Flückiger, J., Monnin, E., Stauffer, B., Schwander, J., Stocker, T. F., Chappellaz, J., Raynaud, D., and Barnola, J. M.: High resolution Holocene $N_2O$ ice core record and its relationship with $CH_4$ and $CO_2$, Global Biogeochem. Cy., 16, 1010, doi:10.1029/2001GB001417, 2002.

Fleitmann, D., Burns, S. J., Mudelsee, M., Neff, U., Kramers, J., Mangini, A., and Matter, A.: Holocene forcing of the Indian monsoon recorded in a stalagmite from Southern Oman, Science, 300, 1737–1739, 2003.

Forster, P., Ramaswamy, V., Artaxo, P., Berntsen, T., Betts, R., Fahey, D. W., Haywood, J., Lean, J., Lowe, D. C., and Myhre, G.: Changes in atmospheric constituents and in radiative forcing, Climatic Change, 20, 129–234, 2007.

Gao, C., Robock, A., Self, S., Witter, J. B., Steffenson, J., Clausen, H. B., Siggard-Andersen, M. L., Johnson, S., Mayewski, P. A., and Ammann, C.: The 1452 or 1453 AD Kuwae eruption signal derived from multiple ice core records: greatest volcanic sulfate event of the past 700 years, J. Geophys. Res.-Atmos., 111, D12107, doi:10.1029/2005JD006710, 2006.

Gao, C., Oman, L., Robock, A., and Stenchikov, G. L.: Atmospheric volcanic loading derived from bipolar ice cores: accounting for the spatial distribution of volcanic deposition, J. Geophys. Res, 112, D09109, doi:10.1029/2006JD007461, 2007.

Gao, C., Robock, A., and Ammann, C.: Volcanic forcing of climate over the past 1500 years: an improved ice core-based index for climate models, J. Geophys. Res.-Atmos., 113, D23111, doi:10.1029/2008JD010239, 2008.

Goujon, C., Barnola, J. M., and Ritz, C.: Modeling the densification of polar firn including heat diffusion: application to close-off characteristics and gas isotopic fractionation for Antarctica and Greenland sites, J. Geophys. Res.-Atmos., 108, 4792, doi:10.1029/2002JD003319, 2003.

Gray, L., Beer, J., Geller, M., Haigh, J., Lockwood, M., Matthes, K., Cubasch, U., Fleitmann, D., Harrison, G., and Hood, L.: Solar influences on climate, Rev. Geophys, 48, G4001, doi:10.1029/2009RG000282, 2010.

Grinsted, A., Moore, J., and Jevrejeva, S.: Nonlinear processes in geophysics application of the cross wavelet transform and wavelet coherence to geophysical time series, Nonlinear Proc. Geophys., 11, 561–566, 2004.





CPD
8, 4817–4883, 2012

Causes of Greenland temperature variability over the past 4000 yr

T. Kobashi et al.

Hanna, E., Jonsson, T., and Box, J. E.: An analysis of Icelandic climate since the nineteenth century, Int. J. Climatol., 24, 1193–1210, 2004.
Hansen, J., Ruedy, R., Sato, M., and Lo, K.: Global surface temperature change, Rev. Geophys, 48, 1–29, 2010.
Hegerl, G. C., Crowley, T. J., Allen, M., Hyde, W. T., Pollack, H. N., Smerdon, J., and Zorita, E.: Detection of human influence on a new, validated 1500-year temperature reconstruction, J. Climate, 20, 650–666, 2007.
Huber, C., Leuenberger, M., Spahni, R., Fluckiger, J., Schwander, J., Stocker, T. F., Johnsen, S., Landals, A., and Jouzel, J.: Isotope calibrated Greenland temperature record over Marine Isotope Stage 3 and its relation to $CH_4$, Earth Planet. Sc. Lett., 243, 504–519, 2006.
Huntley, B.: Reconstructing palaeoclimates from biological proxies: some often overlooked sources of uncertainty, Quaternary Sci. Rev.,31, 1–16, 2011.
Hurrell, J. W.: Decadal trends in the North Atlantic Oscillation: regional temperatures and precipitation, Science, 269, 676–679, 1995.
Hurrell, J. W.: Influence of variations in extratropical wintertime teleconnections on Northern Hemisphere temperature, Geophys. Res. Lett., 23, 665–668, 1996.
Hurrell, J. W., Kushnir, Y., Ottersen, G., and Visbeck, M.: An overview of the North Atlantic oscillation, Geophys. Monogr. AGU, 134, 1–36, 2003.
Ito, H. and Minobe, S.: Data analysis for meteorology and physical oceanography, Meteorological Research Note, 233, Meteorological Society of Japan, Tokyo, 263 pp., 2010.
Jacob, T., Wahr, J., Pfeffer, W. T., and Swenson, S.: Recent contributions of glaciers and ice caps to sea level rise, Nature, 482, 514–518, 2012.
Johnsen, S. J., Dahl Jensen, D., Gundestrup, N., Steffensen, J. P., Clausen, H. B., Miller, H., Masson Delmotte, V., Sveinbjörnsdottir, A. E., and White, J.: Oxygen isotope and palaeotemperature records from six Greenland ice core stations: Camp Century, Dye 3, GRIP, GISP2, Renland and NorthGRIP, J. Quaternary Sci., 16, 299–307, 2001.
Jones, P. D. and Mann, M. E.: Climate over past millennia, Rev. Geophys., 42, RG2002, doi:10.1029/2003RG000143, 2004.
Jouzel, J., Alley, R. B., Cuffey, K. M., Dansgaard, W., Grootes, P., Hoffmann, G., Johnsen, S. J., Koster, R. D., Peel, D., Shuman, C. A., Stievenard, M., Stuiver, M., and White, J.: Validity of the temperature reconstruction from water isotopes in ice cores, J. Geophys. Res.-Oceans, 102, 26471–26487, 1997.

Kaufman, D., Ager, T., Anderson, N., Anderson, P., Andrews, J., Bartlein, P., Brubaker, L., Coats, L., Cwynar, L. C., and Duvall, M.: Holocene thermal maximum in the Western Arctic (0–180° W), Quaternary Sci. Rev., 23, 529–560, 2004.
Kaufman, D. S., Schneider, D. P., McKay, N. P., Ammann, C. M., Bradley, R. S., Briffa, K. R., Miller, G. H., Otto-Bliesner, B. L., Overpeck, J. T., and Vinther, B. M.: Recent warming reverses long-term arctic cooling, Science, 325, 1236–1239, 2009.
Knudsen, M. F., Seidenkrantz, M. S., Jacobsen, B. H., and Kuijpers, A.: Tracking the Atlantic Multidecadal Oscillation through the last 8,000 years, 178, Nat. Commun., 2, 178, 2011.
Kobashi, T.: Greenland temperature, climate change, and human society during the last 11,600 years, PhD thesis, University of California, San Diego, 2007.
Kobashi, T., Severinghaus, J., Brook, E. J., Barnola, J. M., and Grachev, A.: Precise timing and characterization of abrupt climate change 8,200 years ago from air trapped in polar ice, Quaternary Sci. Rev., 26, 1212–1222, doi:10.1016/j.quascirev.2007.01.009, 2007.
Kobashi, T., Severinghaus, J. P., and Barnola, J. M.: $4\pm1.5\,^{\circ}$C abrupt warming 11,270 years ago identified from trapped air in Greenland ice, Earth Planet. Sc. Lett., 268, 397–407, 2008a.
Kobashi, T., Severinghaus, J. P., and Kawamura, K.: Argon and nitrogen isotopes of trapped air in the GISP2 ice core during the Holocene epoch (0–11,600 B.P.): Methodology and implications for gas loss processes, Geochim. Cosmochim. Acta, 72, 4675–4686, 2008b.
Kobashi, T., Severinghaus, J. P., Barnola, J. M., Kawamura, K., Carter, T., and Nakaegawa, T.: Persistent multi-decadal Greenland temperature fluctuation through the last millennium, Climatic Change, 100, 733–756, 2010.
Kobashi, T., Kawamura, K., Severinghaus, J. P., Barnola, J.-M., Nakaegawa, T., Vinther, B. M., Johnsen, S. J., and Box, J. E.: High variability of Greenland surface temperature over the past 4000 years estimated from trapped air in an ice core, Geophys. Res. Lett., 38, L21501, doi:10.1029/2011GL049444, 2011.
Kobashi, T., Shindell, D. T., Kodera, K., Box, J. E., Nakaegawa, T., and Kawamura, K.: On the origin of Greenland temperature anomalies over the past 800 years, J. Geophys. Res., submitted, 2012.
Kodera, K. and Kuroda, Y.: Dynamical response to the solar cycle, J. Geophys. Res., 107, 4749, doi:10.1029/2002JD002224, 2002.
Lal, D. and Peters, B.: Cosmic ray produced radioactivity on the earth, in: Handbuch der Physik, vol. XLVI/2, edited by: Fluegge, S. and Sitte, K., Springer, Berlin, Heidelberg, New York, 551–612, 1968.





CPD
8, 4817–4883, 2012

Lambeck, K. and Chappell, J.: Sea level change through the last glacial cycle, Science, 292, 679–686, 2001.
Landais, A., Caillon, N., Goujon, C., Grachev, A. M., Barnola, J. M., Chappellaz, J., Jouzel, J., Masson-Delmotte, V., and Leuenberger, M.: Quantification of rapid temperature change during DO event 12 and phasing with methane inferred from air isotopic measurements, Earth Planet. Sc. Lett., 225, 221–232, 2004.
Lang, C., Leuenberger, M., Schwander, J., and Johnsen, S.: 16 degrees C rapid temperature variation in Central Greenland 70,000 years ago, Science, 286, 934–937, 1999.
Laskar, J., Robutel, P., Joutel, F., Gastineau, M., Correia, A., and Levrard, B.: A long-term numerical solution for the insolation quantities of the Earth, Astronom. Astrophys., 428, 261–285, 2004.
Lean, J. and Rind, D.: How natural and anthropogenic influences alter global and regional surface temperatures: 1889 to 2006, Geophys. Res. Lett, 35, L18701, doi:10.1029/2008GL034864, 2008.
LeGrande, A. N. and Schmidt, G. A.: Sources of Holocene variability of oxygen isotopes in paleoclimate archives, Clim. Past, 5, 441–455, doi:10.5194/cp-5-441-2009, 2009.
Ljungqvist, F. C., Krusic, P. J., Brattström, G., and Sundqvist, H. S.: Northern Hemisphere temperature patterns in the last 12 centuries, Clim. Past, 8, 227–249, doi:10.5194/cp-8-227-2012, 2012.
Mann, M. E., Bradley, R. S., and Hughes, M. K.: Northern Hemisphere temperatures during the past millennium: inferences, uncertainties, and limitations, Geophys. Res. Lett., 26, 759–762, 1999.
Mann, M. E., Zhang, Z., Hughes, M. K., Bradley, R. S., Miller, S. K., Rutherford, S., and Ni, F.: Proxy-based reconstructions of hemispheric and global surface temperature variations over the past two millennia, Proc. Natl. Acad. Sci. USA, 105, 13252–13257, 2008.
Mann, M. E., Zhang, Z., Rutherford, S., Bradley, R. S., Hughes, M. K., Shindell, D., Ammann, C., Faluvegi, G., and Ni, F.: Global signatures and dynamical origins of the Little Ice Age and Medieval Climate Anomaly, Science, 326, 1256–1260, 2009.
Mann, M. E., Fuentes, J. D., and Rutherford, S.: Underestimation of volcanic cooling in tree-ring-based reconstructions of hemispheric temperatures, Nat. Geosci., 5, 202–205, 2012.
Marshall, J., Kushnir, Y., Battisti, D., Chang, P., Czaja, A., Dickson, R., Hurrell, J., McCartney, M., Saravanan, R., and Visbeck, M.: North Atlantic climate variability: phenomena, impacts and mechanisms, Int. J. Climatol., 21, 1863–1898, 2001.

Martin-Puertas, C., Matthes, K., Brauer, A., Muscheler, R., Hansen, F., Petrick, C., Aldahan, A., Possnert, G., and van Geel, B.: Regional atmospheric circulation shifts induced by a grand solar minimum, Nat. Geosci., 5, 397–401, 2012.

Masson-Delmotte, V., Landais, A., Stievenard, M., Cattani, O., Falourd, S., Jouzel, J., Johnsen, S. J., Jensen, D. D., Sveinsbjørnsdottir, A., White, J. W. C., Popp, T., and Fischer, H.: Holocene climatic changes in Greenland: different deuterium excess signals at Greenland Ice Core Project (GRIP) and NorthGRIP, J. Geophys. Res.-Atmos., 110, D14102, doi:10.1029/2004JD005575, 2005.

Mayewski, P. A., Meeker, L. D., Twickler, M. S., Whitlow, S., Yang, Q. Z., Lyons, W. B., and Prentice, M.: Major features and forcing of high-latitude Northern Hemisphere atmospheric circulation using a 110,000-year-long glaciochemical series, J. Geophys. Res.-Oceans, 102, 26345–26366, 1997.

Mayewski, P. A., Rohling, E. J., Stager, C., Karlen, W., Maasch, K. A., Meeker, L. D., Meyerson, E. A., Gasse, F., van Kreveld, S., Holmgren, K., Lee-Thorp, J., Rosqvist, G., Rack, F., Staubwasser, M., Schneider, R. R., and Steig, E. J.: Holocene climate variability, Quarternary Res., 62, 243–255, 2004.

McCabe, G. J., Palecki, M. A., and Betancourt, J. L.: Pacific and Atlantic Ocean influences on multidecadal drought frequency in the United States, Proc. Natl. Acad. Sci. USA, 101, 4136–4141, 2004.

McGuffie, K. and Henderson-Sellers, A.: A climate modelling primer, Chichester, West Sussex, England, Wiley, 2005.

Meese, D. A., Gow, A., Grootes, P., Stuiver, M., Mayewski, P., Zielinski, G., Ram, M., Taylor, K., and Waddington, E.: The accumulation record from the GISP2 core as an indicator of climate change throughout the Holocene, Science, 266, 1680–1682, 1994.

Moberg, A., Sonechkin, D. M., Holmgren, K., Datsenko, N. M., and Karlen, W.: Highly variable Northern Hemisphere temperatures reconstructed from low- and high-resolution proxy data, Nature, 433, 613–617, 2005.

Monnin, E., Steig, E. J., Siegenthaler, U., Kawamura, K., Schwander, J., Stauffer, B., Stocker, T. F., Morse, D. L., Barnola, J. M., and Bellier, B.: Evidence for substantial accumulation rate variability in Antarctica during the Holocene, through synchronization of $CO_2$ in the Taylor Dome, Dome C and DML ice cores, Earth Planet. Sc. Lett., 224, 45–54, 2004.





CPD
8, 4817–4883, 2012

Causes of Greenland temperature variability over the past 4000 yr

T. Kobashi et al.

Neff, U., Burns, S., Mangini, A., Mudelsee, M., Fleitmann, D., and Matter, A.: Strong coherence between solar variability and the monsoon in Oman between 9 and 6 kyr ago, Nature, 411, 290–293, 2001.

North, G. R., Biondi, F., Bloomfield, P., Christy, J., Cuffey, K., Dickinson, R., Druffel, E., Nychka, D., Otto-Bliesner, B., and Roberts, N.: Surface temperature reconstructions for the last 2,000 years, NRC Statement to Subcommittee on Oversight and Investigations, Committee on Energy and Commerce, US House of Representatives, available at: http://www7.nationalacademies.org/ocga/testimony/Surface_Temperature_Reconstructions.asp, 2006.

Ohmura, A. and Reeh, N.: New precipitation and accumulation maps for Greenland, J. Glaciol, 37, 140–148, 1991.

Otterå, O. H., Bentsen, M., Drange, H., and Suo, L.: External forcing as a metronome for Atlantic multidecadal variability, Nat. Geosci., 3, 688–694, 2010.

Ramaswamy, V., Boucher, O., Haigh, J., Hauglustaine, D., Haywood, J., Myhre, G., Nakajima, T., Shi, G., Solomon, S., and Betts, R. E.: Radiative forcing of climate change, in: Climate Change 2001: The Scientific Basis, Cambridge University Press, New York, 349–416, 2001.

Renssen, H., Goosse, H., and Muscheler, R.: Coupled climate model simulation of Holocene cooling events: oceanic feedback amplifies solar forcing, Clim. Past, 2, 79–90, doi:10.5194/cp-2-79-2006, 2006.

Robock, A.: Volcanic eruptions and climate, Rev. Geophys., 38, 191–219, 2000.

Rogers, J. C., Bolzan, J. F., and Pohjola, V. A.: Atmospheric circulation variability associated with shallow-core seasonal isotopic extremes near Summit, Greenland, J. Geophys. Res., 103, 11, doi:10.1029/98JD00591, 1998.

Schmidt, G. A., Jungclaus, J. H., Ammann, C. M., Bard, E., Braconnot, P., Crowley, T. J., Delaygue, G., Joos, F., Krivova, N. A., Muscheler, R., Otto-Bliesner, B. L., Pongratz, J., Shindell, D. T., Solanki, S. K., Steinhilber, F., and Vieira, L. E. A.: Climate forcing reconstructions for use in PMIP simulations of the Last Millennium (v1.1), Geosci. Model Dev., 5, 185–191, doi:10.5194/gmd-5-185-2012, 2012.

Sellers, W. D.: A global climatic model based on the energy balance of the Earth-atmosphere system, J. Appl. Meteorol., 8, 392–400, 1969.

Severinghaus, J. P. and Brook, E. J.: Abrupt climate change at the end of the last glacial period inferred from trapped air in polar ice, Science, 286, 930–934, 1999.

Severinghaus, J. P., Sowers, T., Brook, E. J., Alley, R. B., and Bender, M. L.: Timing of abrupt climate change at the end of the Younger Dryas interval from thermally fractionated gases in polar ice, Nature, 391, 141–146, 1998.
Shindell, D. T., Schmidt, G. A., Mann, M. E., Rind, D., and Waple, A.: Solar forcing of regional climate change during the Maunder Minimum, Science, 294, 2149–2152, 2001.
Solomon, S., Qin, D., Manning, M., Chen, Z., Marquis, M., Averyt, K., Tignor, M., and Miller, H.: Climate change 2007: the Physical Science Basis, Contribution of Working Group I to the Fourth Assessment Report of the Intergovernmental Panel on Climate Change, 2007.
Spahni, R., Schwander, J., Flückiger, J., Stauffer, B., Chappellaz, J., and Raynaud, D.: The attenuation of fast atmospheric $CH_4$ variations recorded in polar ice cores, Geophys. Res. Lett., 30, 1571, doi:10.1029/2003GL017093, 2003.
Steen-Larsen, H., Masson-Delmotte, V., Sjolte, J., Johnsen, S., Vinther, B., Bréon, F. M., Clausen, H., Dahl-Jensen, D., Falourd, S., and Fettweis, X.: Understanding the climatic signal in the water stable isotope records from the NEEM shallow firn/ice cores in Northwest Greenland, J. Geophys. Res., 116, D06108, doi:10.1029/2010JD014311, 2011.
Steinhilber, F., Beer, J., and Frlich, C.: Total solar irradiance during the Holocene, Geophys. Res. Lett., 36, L19704, doi:10.1029/2009GL040142, 2009.
Steinhilber, F., Abreu, J. A., Beer, J., Brunner, I., Christl, M., Fischer, H., Heikkilä, U., Kubik, P. W., Mann, M., and McCracken, K. G.: 9,400 years of cosmic radiation and solar activity from ice cores and tree rings, Proc. Natl. Acad. Sci. USA, 109, 5967–5971, 2012.
Stothers, R. B.: The great Tambora eruption in 1815 and its aftermath, Science, 224, 1191–1198, 1984.
Stuiver, M., Grootes, P. M., and Braziunas, T. F.: The GISP2 delta O-18 climate record of the past 16,500 years and the role of the sun, ocean, and volcanoes, Quaternary Res., 44, 341–354, 1995.
Stuiver, M., Braziunas, T., Grootes, P., and Zielinski, G.: Is there evidence for solar forcing of climate in the GISP2 oxygen isotope record?, Quaternary Res., 48, 259–266, 1997.
Usoskin, I. G., Horiuchi, K., Solanki, S., Kovaltsov, G. A., and Bard, E.: On the common solar signal in different cosmogenic isotope data sets, J. Geophys. Res, 114, A03112, doi:10.1029/2008JA013888, 2009.
Vieira, L. E. A., Solanki, S. K., Krivova, N. A., and Usoskin, I.: Evolution of the solar irradiance during the Holocene, 531, A6, doi:10.1051/0004-6361/201015843, 2011.





CPD
8, 4817–4883, 2012

Causes of Greenland temperature variability over the past 4000 yr

T. Kobashi et al.

Vinther, B. M., Johnsen, S. J., Andersen, K. K., Clausen, H. B., and Hansen, A. W.: NAO signal recorded in the stable isotopes of Greenland ice cores, Geophys. Res. Lett, 30, 1387, doi:10.1029/2002GL016193, 2003.

Vinther, B. M., Clausen, H. B., Johnsen, S. J., Rasmussen, S. O., Andersen, K. K., Buchardt, S. L., Dahl-Jensen, D., Seierstad, I. K., Siggaard-Andersen, M. L., Steffensen, J. P., Svensson, A., Olsen, J., and Heinemeier, J.: A synchronized dating of three Greenland ice cores throughout the Holocene, J. Geophys. Res.-Atmos., 111, D13102, doi:10.1029/2005JD006921, 2006.

Vinther, B. M., Clausen, H. B., Fisher, D., Koerner, R., Johnsen, S. J., Andersen, K. K., Dahl-Jensen, D., Rasmussen, S. O., Steffensen, J. P., and Svensson, A.: Synchronizing ice cores from the Renland and Agassiz ice caps to the Greenland ice core chronology, J. Geophys. Res, 113, D08115, doi:10.1029/2007JD009143, 2008.

Vinther, B. M., Buchardt, S. L., Clausen, H. B., Dahl-Jensen, D., Johnsen, S. J., Fisher, D. A., Koerner, R. M., Raynaud, D., Lipenkov, V., Andersen, K. K., Blunier, T., Rasmussen, S. O., Steffensen, J. P., and Svensson, A. M.: Holocene thinning of the Greenland ice sheet, Nature, 461, 385–388, 2009.

Vinther, B. M., Jones, P. D., Briffa, K. R., Clausen, H. B., Andersen, K. K., DahlJensen, D., and Johnsen, S. J.: Climatic signals in multiple highly resolved stable isotope records from Greenland, Quarternary Sci. Rev., 29, 522–538, 2010.

Wang, Y. J., Cheng, H., Edwards, R. L., He, Y. Q., Kong, X. G., An, Z. S., Wu, J. Y., Kelly, M. J., Dykoski, C. A., and Li, X. D.: The Holocene Asian monsoon: links to solar changes and North Atlantic climate, Science, 308, 854–857, 2005a.

Wang, Y. M., Lean, J., and Sheeley Jr, N.: Modeling the sun's magnetic field and irradiance since 1713, Astrophys. J., 625, doi:10.1086/429689, 2005b.

Wanner, H., Brönnimann, S., Casty, C., Gyalistras, D., Luterbacher, J., Schmutz, C., Stephenson, D. B., and Xoplaki, E.: North Atlantic Oscillation – concepts and studies, Surv. Geophys., 22, 321–381, 2001.

Wanner, H., Beer, J., Butikofer, J., Crowley, T. J., Cubasch, U., Fluckiger, J., Goosse, H., Grosjean, M., Joos, F., Kaplan, J. O., Kuttel, M., Muller, S. A., Prentice, I. C., Solomina, O., Stocker, T. F., Tarasov, P., Wagner, M., and Widmann, M.: Mid- to late Holocene climate change: an overview, Quarternary Sci. Rev., 27, 1791–1828, 2008.

Wanner, H., Solomina, O., Grosjean, M., Ritz, S. P., and Jetel, M.: Structure and origin of Holocene cold events, Quaternary Sci. Rev., 30, 3109–3123, 2011.

Warren, S. G. and Schneider, S. H.: Seasonal simulation as a test for uncertainties in the parameterizations of a Budyko-Sellers zonal climate model, J. Atmos. Sci., 36, 1377–1391, 1979.
Werner, M., Heimann, M., and Hoffmann, G.: Isotopic composition and origin of polar precipitation in present and glacial climate simulations, Tellus B, 53, 53–71, 2001.
White, J. W. C., Barlow, L. K., Fisher, D., Grootes, P., Jouzel, J., Johnsen, S. J., Stuiver, M., and Clausen, H.: The climate signal in the stable isotopes of snow from Summit, Greenland: results of comparisons with modern climate observations, J. Geophys. Res.-Oceans, 102, 26425–26439, 1997.
Wigley, T., Ammann, C., Santer, B., and Raper, S. C. B.: Effect of climate sensitivity on the response to volcanic forcing, J. Geophys. Res, 110, D09107, doi:10.1029/2004JD005557, 2005.
Zielinski, G. A.: Stratospheric loading and optical depth estimates of explosive volcanism over the last 2100 years derived from the Greenland Ice Sheet Project 2 ice core, J. Geophys. Res., 100, 20937–20955, 1995.
Zielinski, G. A., Mayewski, P. A., Meeker, L. D., Whitlow, S., Twickler, M. S., Morrison, M., Meese, D. A., Gow, A. J., and Alley, R. B.: Record of volcanism since 7000 BC from the GISP2 Greenland ice core and implications for the volcano-climate system, Science, 264, 948–952, 1994.

**Table 1.** Characteristics of the current climate in six core sites. The data from NGRIP, GRIP, and Renland are from Vinther et al. (2008); data for Dye-3 are from Vinther et al. (2006); and data for GISP2 are from Meese et al. (1994) and Kobashi et al. (2011).

| Ice Cores | Elevation (m a.s.l.) | Latitude (°N) | Longitude (°W) | Mean air temperature (°C) | Accumulation (m ice per year) |
|---|---|---|---|---|---|
| Agassiz 84/87 | 1730 | 80.7 | 73.1 | −21.9 | 0.10 |
| NGRIP | 2920 | 75.1 | 42.3 | −32 | 0.19 |
| GISP2 | 3200 | 72.6 | 38.5 | −30 | 0.21 |
| GRIP | 3230 | 72.6 | 37.6 | −32 | 0.23 |
| Renland | 2350 | 71.3 | 26.7 | −18 | 0.50 |
| Dye-3 | 2490 | 65.2 | 43.8 | −20 | 0.56 |





CPD
8, 4817–4883, 2012

**Table 2.** Correlation coefficient matrix of $\delta^{18}O_{ice}$ with PCAs in 20-yr RMs with solar (raw data) and temperature (raw data). Parentheses indicate *p*-values lower than 0.1 (using a two-sided Student's t-test). Bold text indicates a greater than 90 % confidence level and italic text indicates a greater than 95 % confidence level.

| | GISP2 | GRIP | NGRIP | Renland | Agassiz | Solar | Temp |
|---|---|---|---|---|---|---|---|
| Dye3 | ***0.31*** (< 0.01) | ***0.38 (0.02)*** | ***0.37 (0.01)*** | **0.31 (0.06)** | **0.26 (0.09)** | ***0.28 (0.03)*** | ***0.25 (0.04)*** |
| GISP2 | | ***0.26 (0.05)*** | **0.22 (0.06)** | 0.19 | ***0.3 (0.04)*** | 0.16 | ***0.27 (0.02)*** |
| GRIP | | | **0.51 (0.06)** | 0.42 | 0.33 | 0.24 | 0.34 |
| NGRIP | | | | **0.42 (0.10)** | 0.31 | 0.20 | ***0.39 (0.01)*** |
| Renland | | | | | 0.33 | ***0.34 (0.03)*** | ***0.38 (0.05)*** |
| Agassiz | | | | | | 0.29 | 0.30 |
| PC1 | | | | | | **0.37 (0.10)** | ***0.49 (0.05)*** |
| PC2 | | | | | | 0.00 | −0.02 |
| PC3 | | | | | | −0.07 | −0.06 |
| PC4 | | | | | | 0.12 | −0.07 |
| PC5 | | | | | | 0.11 | 0.04 |
| PC6 | | | | | | −0.04 | 0.07 |





CPD
8, 4817–4883, 2012

**Table 3.** Principal component analysis of oxygen isotopes in ice over the past 4000 yr. Data from $\delta^{18}O_{ice}$ in 20-yr RMs are used for the calculation. Note that initially PC1 had negative correlations with all $\delta^{18}O_{ice}$, but the sign of PC1 is reversed so that PC1 has positive correlations with all $\delta^{18}O_{ice}$, making the discussion simpler.

| | PC1 | PC2 | PC3 | PC4 | PC5 | PC6 |
|---|---|---|---|---|---|---|
| Component loadings | | | | | | |
| Agassiz | 0.38 | 0.27 | −0.73 | 0.40 | −0.29 | −0.01 |
| Dye3 | 0.40 | 0.14 | 0.60 | 0.67 | 0.07 | −0.03 |
| GISP2 | 0.32 | 0.78 | 0.11 | −0.47 | 0.19 | 0.08 |
| GRIP | 0.46 | −0.24 | 0.10 | −0.32 | −0.30 | −0.73 |
| NGRIP | 0.45 | −0.33 | 0.12 | −0.25 | −0.38 | 0.68 |
| Renland | 0.42 | −0.36 | −0.25 | −0.04 | 0.80 | 0.03 |
| Component variance | | | | | | |
| | 2.65 | 0.90 | 0.76 | 0.61 | 0.59 | 0.49 |
| Importance of components | | | | | | |
| Standard deviation | 1.63 | 0.95 | 0.87 | 0.78 | 0.77 | 0.70 |
| Proportion of variance | 0.44 | 0.15 | 0.13 | 0.10 | 0.10 | 0.08 |
| Cumulative proportion | 0.44 | 0.59 | 0.72 | 0.82 | 0.92 | 1 |





CPD
8, 4817–4883, 2012

**Table 4.** Seventeen periods of strong volcanic events over the past 4000 yr. Positive and negative years indicate C.E. and B.C.E., respectively. Average forcing has a unit of $W m^{-2}$.

| # | Starting | Ending | Duration (year) | Ave. forcing ($W m^{-2}$) |
|---|---|---|---|---|
| 1 | 1758 | 1860 | 102 | −0.35 |
| 2 | 1618 | 1668 | 50 | −0.40 |
| 3 | 1437 | 1487 | 50 | −0.25 |
| 4 | 1326 | 1376 | 50 | −0.23 |
| 5 | 1246 | 1297 | 51 | −0.22 |
| 6 | 1161 | 1238 | 77 | −0.20 |
| 7 | 1099 | 1148 | 49 | −0.20 |
| 8 | 930 | 980 | 50 | −0.41 |
| 9 | 612 | 661 | 49 | −0.22 |
| 10 | −81 | −30 | 51 | −0.18 |
| 11 | −201 | −151 | 50 | −0.18 |
| 12 | −432 | −382 | 50 | −0.36 |
| 13 | −639 | −563 | 76 | −0.66 |
| 14 | −1109 | −1059 | 50 | −0.16 |
| 15 | −1211 | −1161 | 50 | −0.22 |
| 16 | −1480 | −1427 | 53 | −0.21 |
| 17 | −1718 | −1593 | 125 | −0.35 |





CPD
8, 4817–4883, 2012

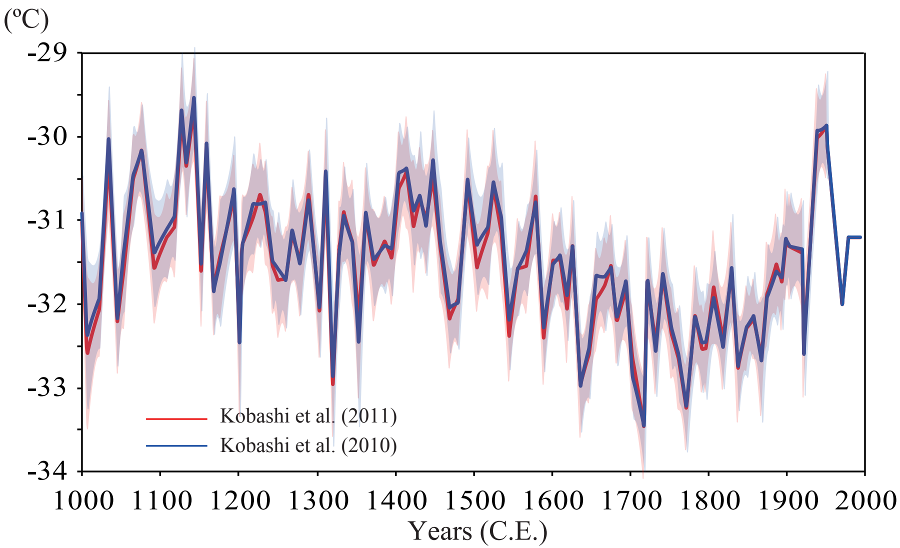


**Fig. 1.** Greenland temperature reconstructions over the past 1000 years from two studies (Kobashi et al., 2010, 2011). Error bands (blue and red) are 1$\sigma$ values. Note that overlapping areas of uncertainties are shown in grey.





CPD
8, 4817–4883, 2012

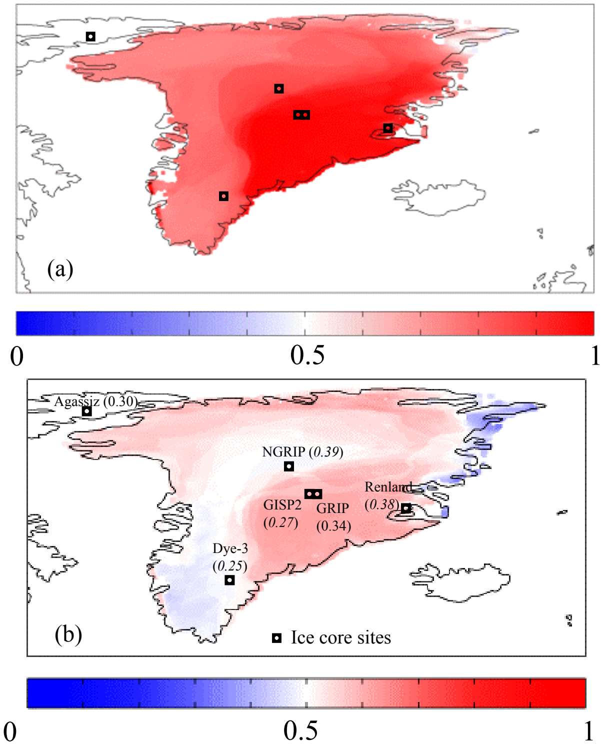


**Fig. 2.** Correlation maps between two Greenland Summit temperatures and grid temperatures over the period from 1852–2010. Grid temperature data are from Box et al. (2009). **(a)** Correlation map with the observation-model-based Summit temperatures (annual resolution) by Box et al. (2009). **(b)** Correlation map with the ice-core-based Summit temperature (raw data) by Kobashi et al. (2011). Grid temperatures are at annual resolution. Parentheses indicate correlation coefficients between the Summit temperatures (Kobashi et al., 2011) and $\delta^{18}O_{ice}$ from six ice cores over the past 4000 yr. Italics represent correlation coefficients with confidence levels of greater than 90 %. See Table 2.





CPD
8, 4817–4883, 2012

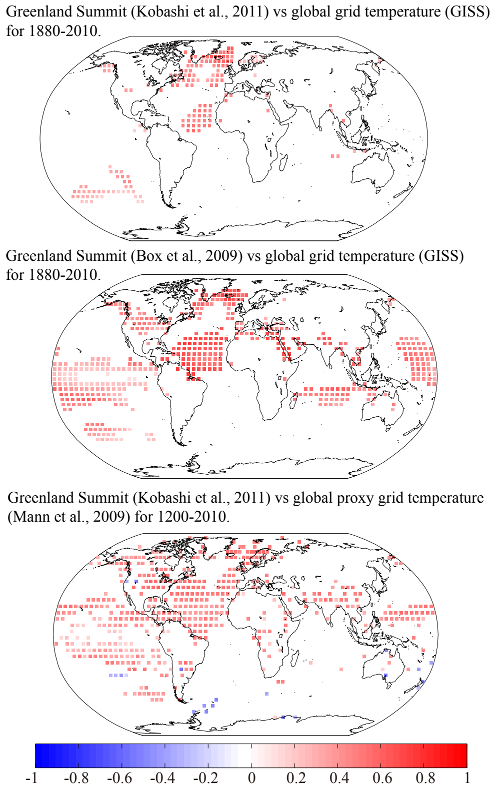


**Fig. 3.** Grid correlation coefficients between two Greenland Summit temperatures (Box et al., 2009; Kobashi et al., 2011) and global grid temperatures (Mann et al., 2009) for two periods from 1880–2010 (top and middle) and 1200–2010 (bottom), respectively. Only grids with > 90 % confidence are shown (two-sided tests). Grids with continuous temperature data for 131 yr (top and middle) and 811 yr (bottom) were used for the calculations, respectively.





CPD
8, 4817–4883, 2012

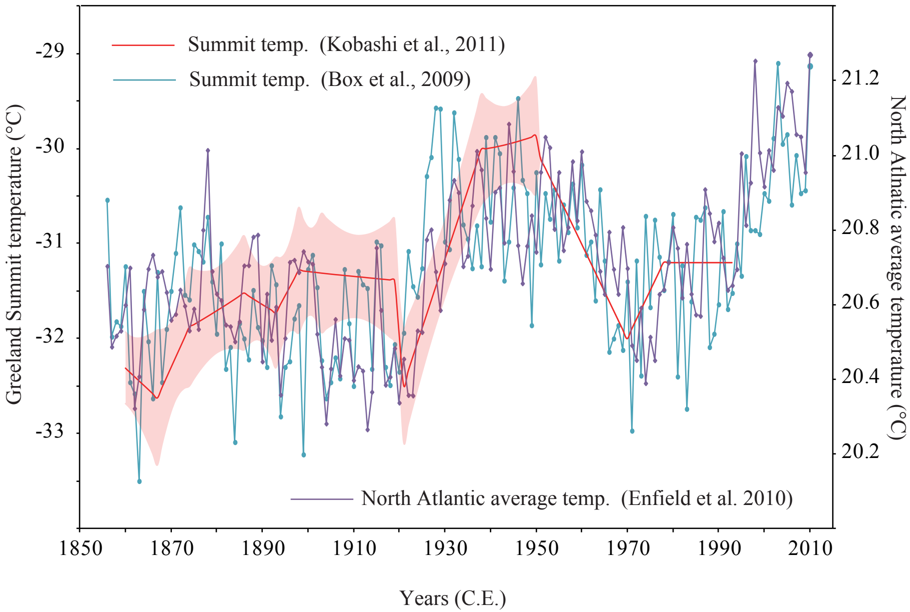


**Fig. 4.** North Atlantic average temperatures (Enfield et al., 2001) and Greenland Summit temperatures (Box et al., 2009; Kobashi et al., 2011). Error band (red) is 1$\sigma$ (Kobashi et al., 2011). The Summit temperature by Box et al. (2009) was shifted by $-1.75\,^{\circ}\mathrm{C}$ to account for the air-surface temperature difference (Kobashi et al., 2011).





CPD
8, 4817–4883, 2012

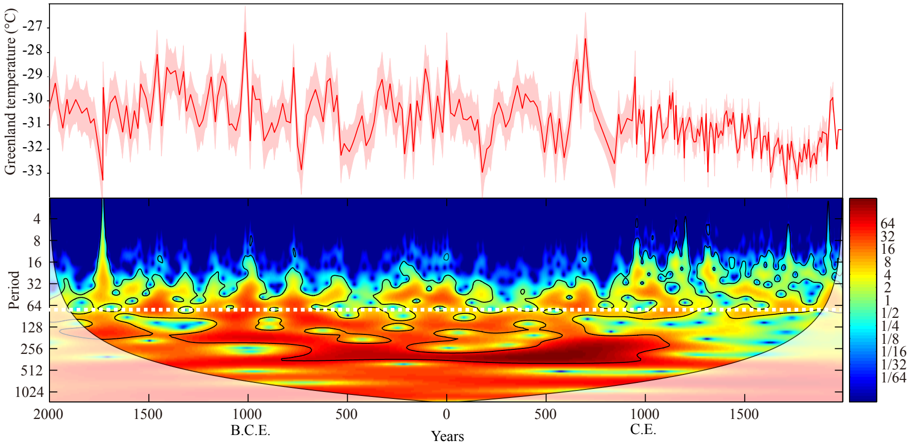


**Fig. 5.** Wavelet analysis (Grinsted et al., 2004) of Greenland temperatures (Kobashi et al., 2011) over the past 4000 yr. The white dotted line indicates the 70 yr periodicity. The area between the grey lines represents the 95 % confidence level relative to the noise (red). Shaded areas represent the cone of influence where edge effects may distort the results. Error bards in the top panel are 1$\sigma$.





CPD
8, 4817–4883, 2012

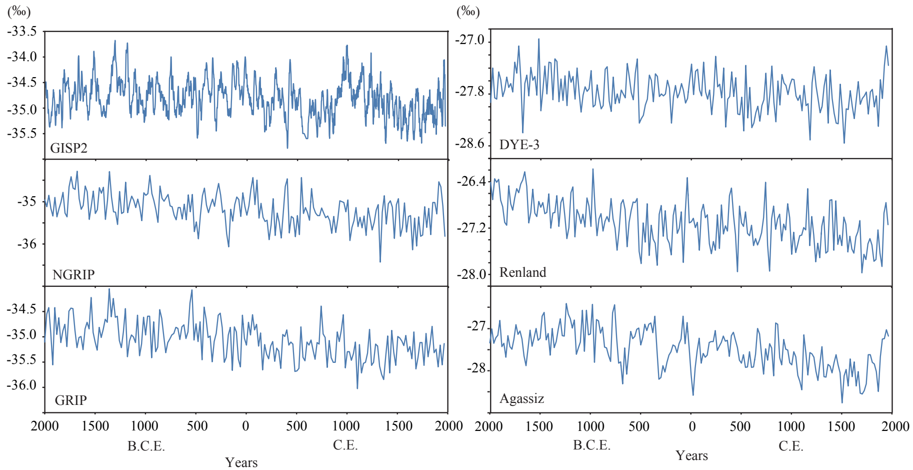


**Fig. 6.** $\delta^{18}O_{ice}$ of the six ice cores from the Greenland region in 20-yr RMs over the past 4000 yr. The GISP2 record is from Stuiver et al. (1995), and the GRIP, NGRIP, DYE-3, Renland, and Agassiz records are from Vinther et al. (2009).





CPD
8, 4817–4883, 2012

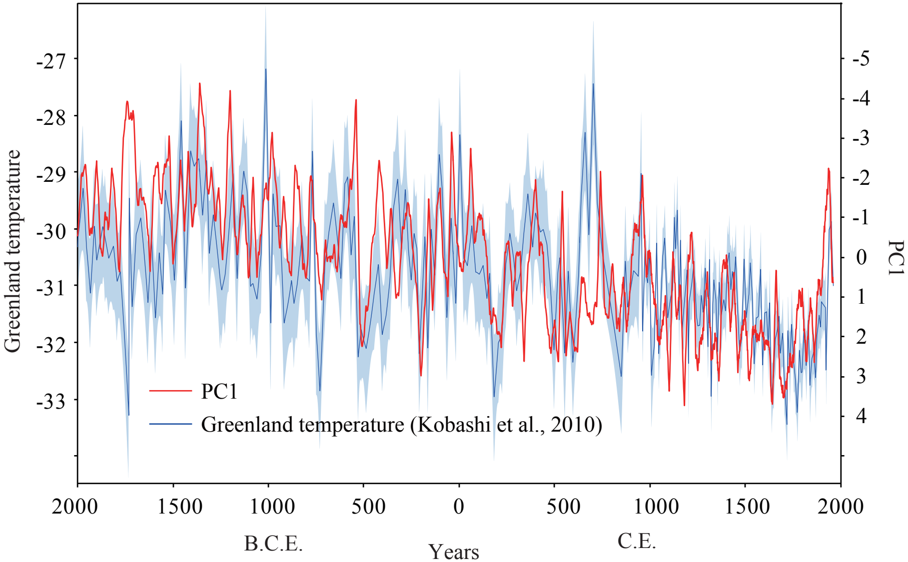


**Fig. 7.** Greenland temperature and PC1 of $\delta^{18}O_{ice}$ of six Greenland ice cores in 20-yr RMs. Blue and red lines represent Greenland temperatures and PC1, respectively. Error bands for Greenland temperature are $1\sigma$.





CPD
8, 4817–4883, 2012

Causes of Greenland temperature variability over the past 4000 yr

T. Kobashi et al.

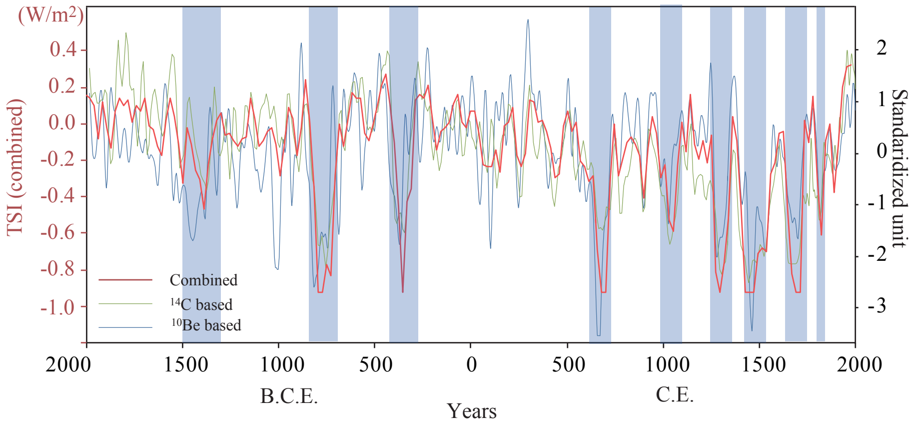


**Fig. 8.** Differences in TSI over the past 4000 yr from the value of 1365.57 $W m^{-2}$ in 1986. The data for combined, $^{14}C$-based, and $^{10}Be$-based estimates are from Steinhilber et al. (2009, 2012), and Vieira et al. (2011), respectively.

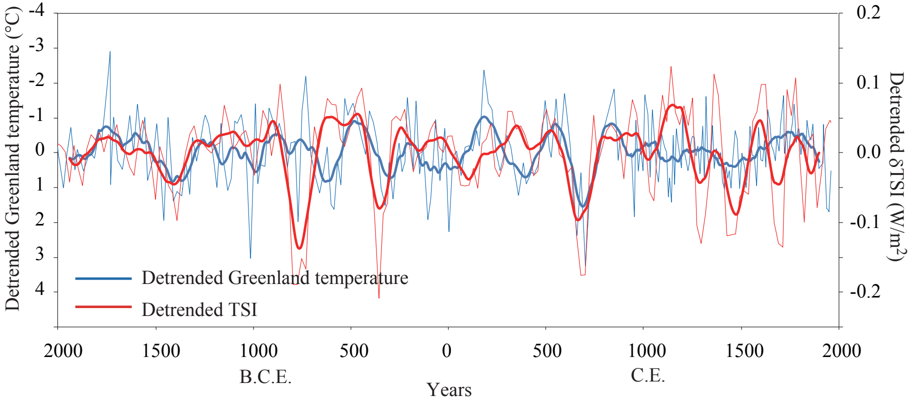


**Fig. 9.** Changes in the detrended solar activity and Greenland temperatures over the past 4000 yr. A high-pass LOESS filter to remove signals longer than 1150 yr was used for detrending (see text). Note that the y-axis for the Greenland temperatures is reversed. Thin and thick lines represent detrended raw data and the data smoothed by the 120 yr RMs, respectively.





CPD
8, 4817–4883, 2012

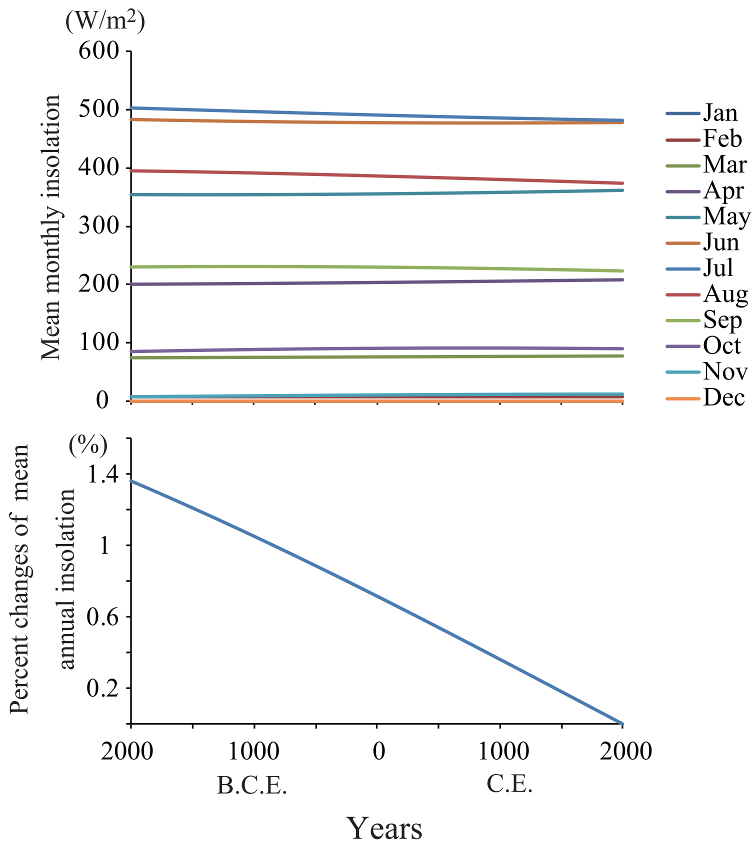


**Fig. 10.** Orbital forcing at 72° N. (top) Mean monthly average insolation. Months are defined from the days 21–20 (e.g. January is from 21 December to 20 January). (bottom) Percent change of mean annual insolation from present. Data are from Laskar et al. (2004). Present mean annual insolation is 192.8 W m$^{-2}$. Note that December and January have no insolation.





CPD
8, 4817–4883, 2012

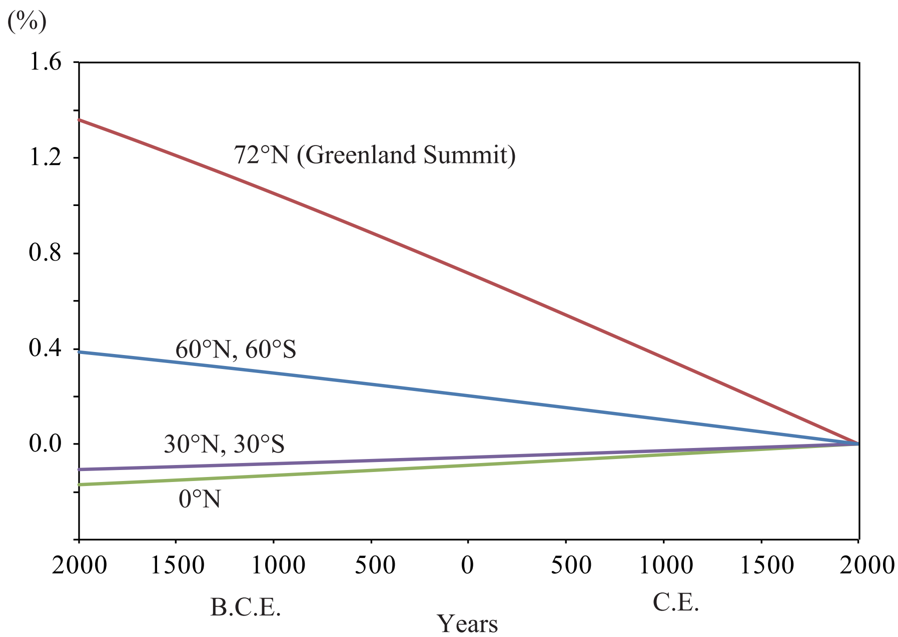


**Fig. 11.** Percent change of annual solar insolation (Laskar et al., 2004) from present in various latitudes over the past 4000 yr.





CPD
8, 4817–4883, 2012

Causes of Greenland temperature variability over the past 4000 yr

T. Kobashi et al.

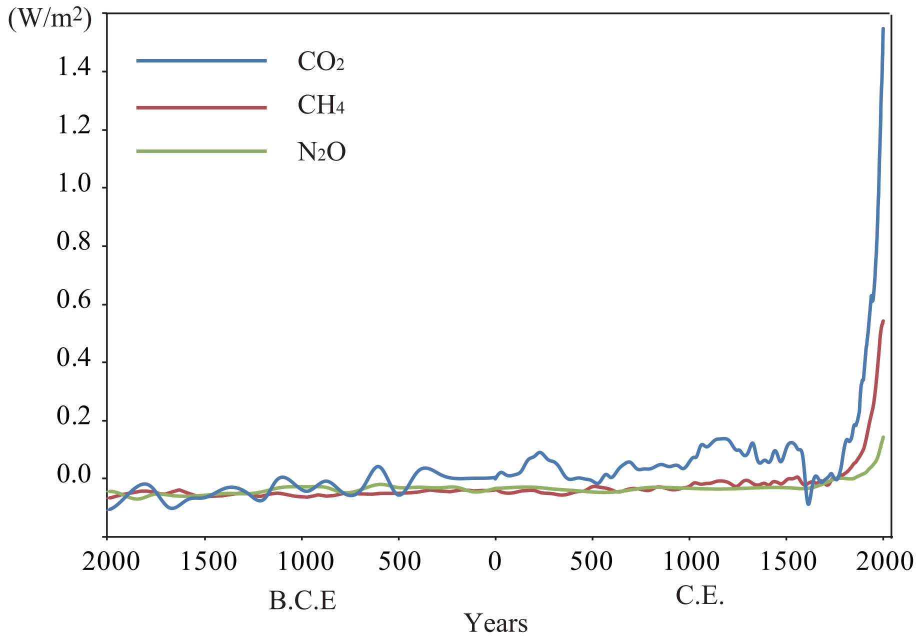


**Fig. 12.** Greenhouse gas forcings by $CO_2$, $CH_4$, and $N_2O$ from 2000 B.C.E to 2000 C.E. The values at 1750 C.E. were set as zeros. See text for the data sources.





CPD
8, 4817–4883, 2012

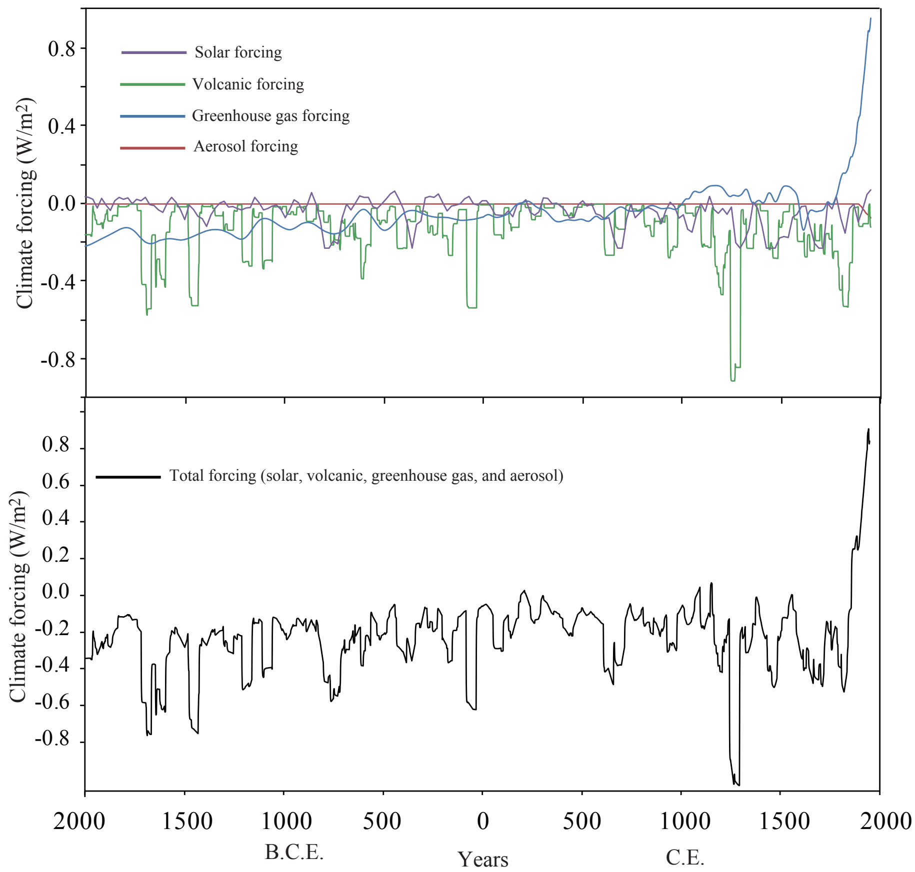


**Fig. 13.** Climate forcings from 2000 B.C.E. to 1950 C.E. (top) Solar, volcanic, greenhouse gas, and aerosol forcings (see text). (bottom) Total climate forcings without orbital forcing.





CPD
8, 4817–4883, 2012

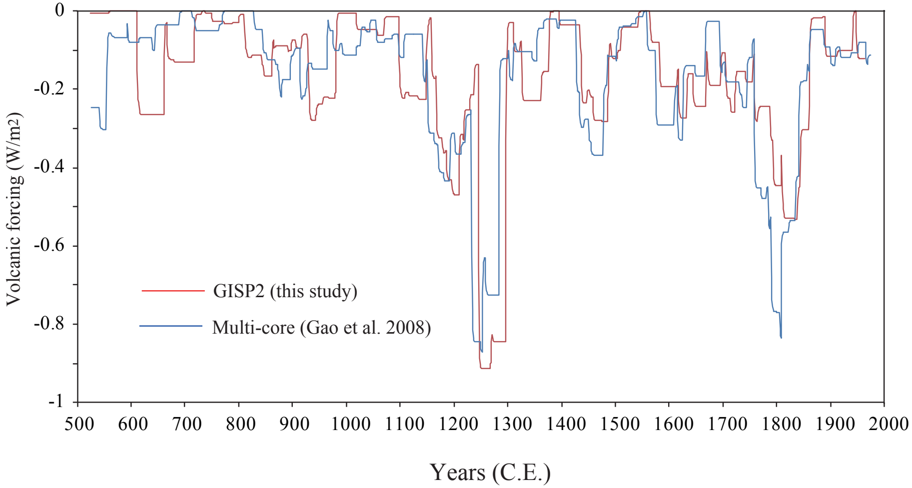


**Fig. 14.** Reconstructed volcanic forcing over the past 1500 yr on the multi-decadal time scale. Red and blue lines represent volcanic forcing reconstructions from a single core (GISP2, this study) and multi-cores (Gao et al., 2008).





CPD
8, 4817–4883, 2012

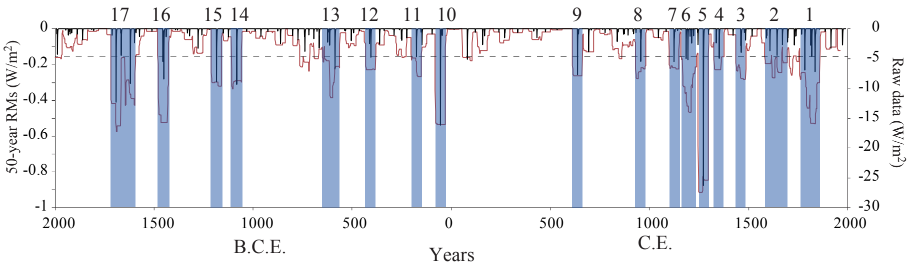


**Fig. 15.** Volcanic forcing for NH over the past 4000 yr derived from the GISP2 sulfate record (Mayewski et al., 1997). Black and red lines are raw data and 51-yr RMs for reconstructed volcanic signals, respectively. Blue shaded areas are periods when volcanic forcings were lower than the standard deviation ($-0.15\,\mathrm{W\,m^{-2}}$; dotted line) of the 51-yr RMs and lasted for more than 50 yr. Seventeen volcanically active periods were identified (Table 4).





CPD
8, 4817–4883, 2012

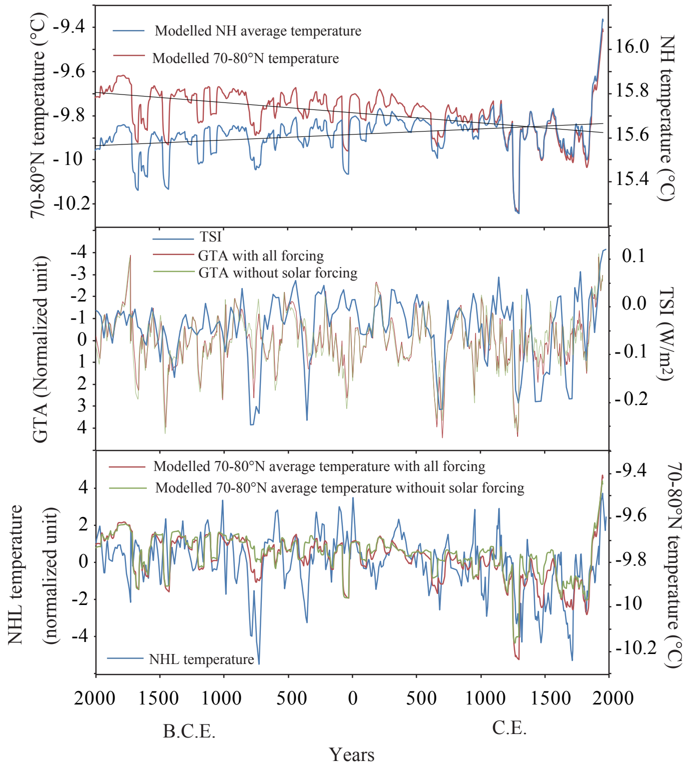


**Fig. 16.** Modeled and ice core-derived temperatures and GTA over the past 4000 yr. (top) Model outputs of NH and 70–80° N average temperatures. Black lines indicate long-term trends over the past 4000 years. (middle) Blue, red, and green lines are the detrended TSI and GTAs calculated with model 70–80° N temperatures with all forcing and without solar forcing, respectively. (bottom) Red, green, and blue lines are modelled 70–80° N temperatures with all forcing and without solar forcing and NHL temperature, respectively.

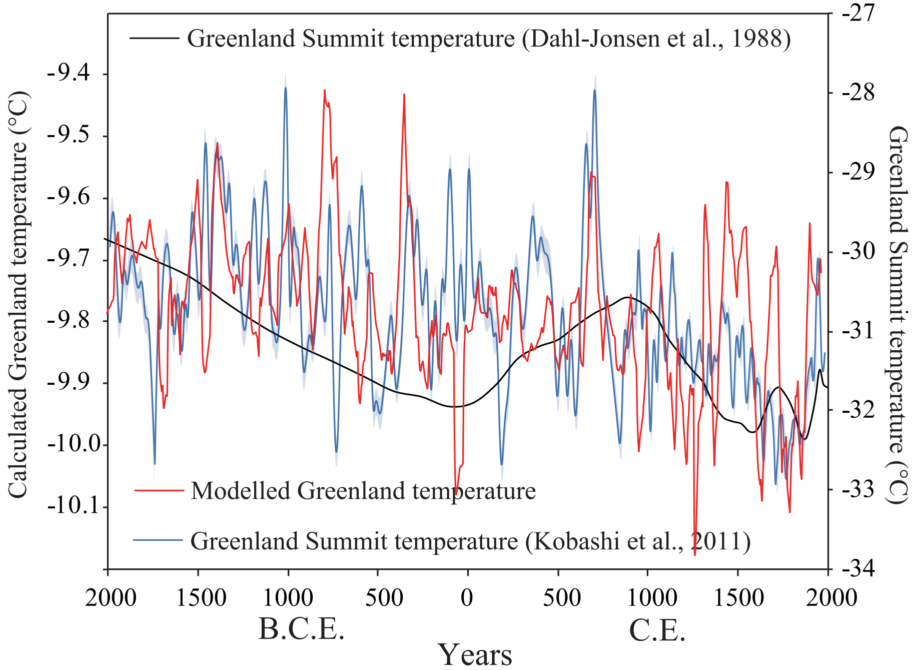


**Fig. 17.** Modeled, ice core-derived (21 yr RMs), and borehole temperature-based Greenland temperatures. Two time series (blue and red) are correlated ($r = 0.32$) at the 97 % confidence level. The black line is Greenland temperature reconstruction from borehole temperature profiles (Dahl-Jensen et al., 1998). $1\sigma$ error bands for the Greenland temperatures in the 21 yr RMs were estimated by a Monte Carlo method following Kobashi et al. (2012).





CPD
8, 4817–4883, 2012

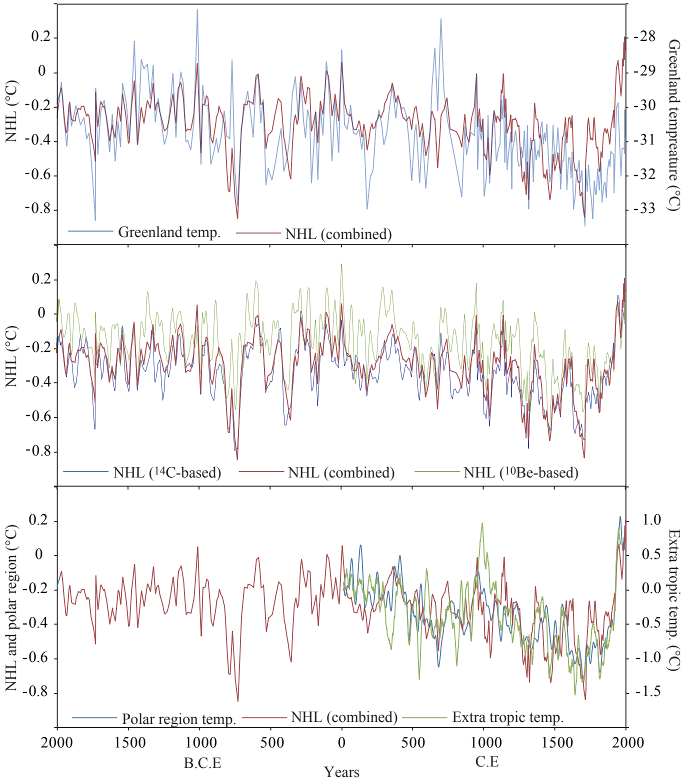


**Fig. 18.** Greenland, NHL, extra-tropical, and polar region temperatures over the past 4000 yr. (top) ice core-derived Greenland temperature (Kobashi et al., 2011) and the NHL temperature. (middle) The NHL temperature derived from different TSI reconstructions (see text). (bottom) The NHL temperature (combined), extra-tropic temperature in 21-yr RMs (Christiansen and Ljungqvist, 2012), and polar region temperature in 21 yr RMs (Kaufman et al., 2009).





CPD
8, 4817–4883, 2012

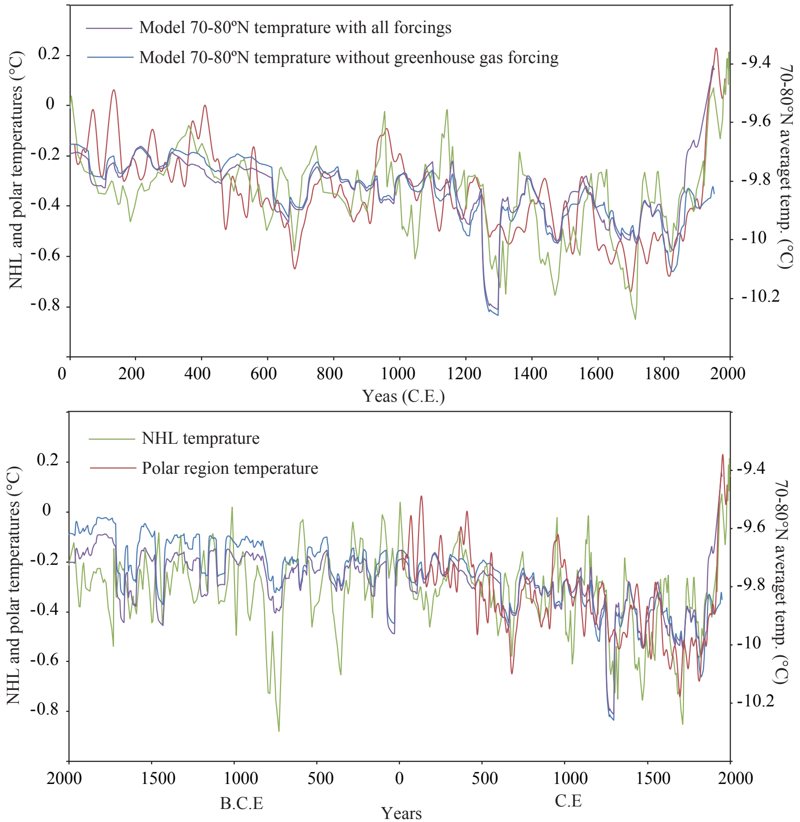


**Fig. 19.** NHL temperature and polar region temperature in 21-yr RMs compared with model outputs for 70–80° N average temperatures with all forcings and without greenhouse gas forcing over the past 4000 yr. (top) Period from 1 C.E. to 2000 C.E. (bottom) Period from 2000 B.C.E to 2000 C.E.

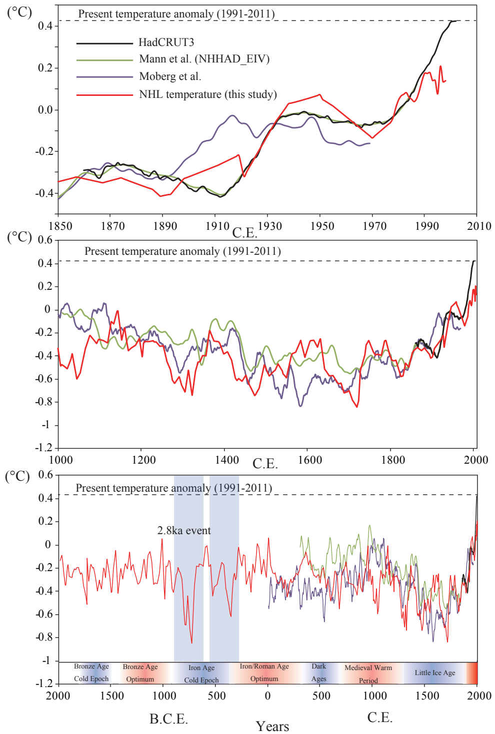


**Fig. 20.** NH temperature anomaly reconstruction (from the base year of 1961–1990). (top) Period from 1850 C.E. to 2010 C.E. (middle) Period from 1000 C.E. to 2010 C.E. (bottom) Period from 2000 B.C.E–2000 C.E. Observed temperatures and the two proxy temperatures are from Brohan et al. (2006), Mann et al. (2008), and Moberg et al. (2005), respectively. These data were smoothed by 21-yr RMs. The present temperature anomaly (dotted line; 0.42 °C) was derived from an average of the NH temperature anomaly (Brohan et al., 2006) from 1991 C.E. to 2011 C.E. Shaded areas in the bottom panel are the 2.8 ka and subsequent cooling events. European cultural climatic zones are also shown in the bottom panel.

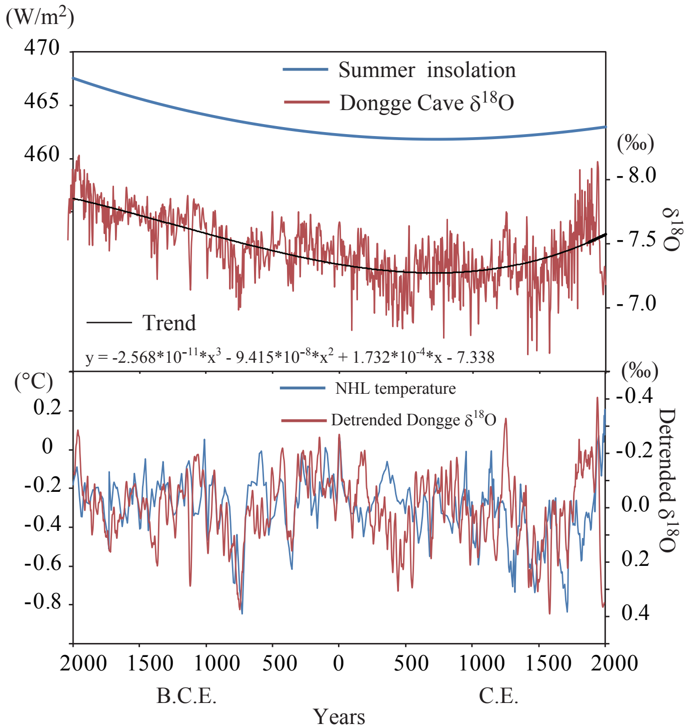


**Fig. 21.** Summer insolation, Dongge Cave spelotherm $\delta^{18}$O, and the NHL temperature. (top) Summer insolation is average insolation of 65° N in June (21 May to 20 June) (Laskar et al., 2004). The Dongge Cave speleotherm $\delta^{18}$O data are from Wang et al. (2005a). The trend line was derived from a polynomial fit (the equation is shown in the upper panel.). (bottom) NHL temperature and detrended Dongge $\delta^{18}$O in 21 RMs that was obtained by subtracting the trend line.





CPD
8, 4817–4883, 2012